UNIVERSITY OF CALIFORNIA
SANTA CRUZ

SPATIO-TEMPORAL CONNECTOME DATA ANALYSIS USING MACHINE LEARNING AND VISUALIZATION

A dissertation submitted in partial satisfaction of the
requirements for the degree of

DOCTOR OF PHILOSOPHY

in

TECHNOLOGY AND INFORMATION MANAGEMENT

by

Ran Xu

June 2022

The Dissertation of Ran Xu
is approved:

Professor Angus G. Forbes, Chair

Professor David T. Lee

Professor Subhas Desa

Professor Olusola A. Ajilore

Peter Biehl
Vice Provost and Dean of Graduate Studies

Table of Contents

List of Figures

List of Tables

Abstract

Spatio-Temporal Connectome Data Analysis using Machine Learning and Visualization

by

Ran Xu

Analysis and comparison of multiple time-varying connectomes is crucial for studying brain diseases such as Depression and Alzheimer's Disease. Recently, many visualization techniques have been proposed to assist clinical psychiatrists in exploring complex connectome datasets but majority of them are focused on static connectome features. We develop two novel visualization applications: *TempoCave* and *ConnectoVis*, for analyzing dynamic brain networks, or connectomes. *TempoCave* and *ConnectoVis* provide a range of functionality to explore metrics related to the activity patterns of different regions in the brain. Analysis of temporal connectome is limited due to high dimensionality of the data. To address this problem, we introduce a new data analysis technique that is specifically designed for dynamic functional connectomes by combining a novel temporal graph neural network and a learnable mask mechanism. Our technique can classify remitted depression group vs control group with 98% accuracy and the mask is used to identify the significant brain regions that contribute to depression. Along with our visualization tools, we have a spatio-temporal connectome analysis pipeline. We demonstrate the effectiveness of our pipeline through three use cases.

This dissertation is dedicated to my parents and sister,

Dongchao Xu, Shuxia Zhao, and Ning Xu.

For their unconditional love, support and encourage.

Acknowledgments

Firstly, I would like to acknowledge the dedication of my advisor, Professor Angus Forbes, who has been patient and caring throughout my PhD research. Angus is the one who provided me the opportunity to work on this thesis. I am very grateful for the knowledge and wisdom he had shared with me.

Additionally, I would like to acknowledge the other members of my committee, Professor Subhas Desa of UCSC TIM department, Professor David Lee of UCSC CM department and Professor Olusola A. Ajilore of UIC Department of Psychiatry, who provided invaluable advice during the course of this research. I greatly appreciate the time they have spent reading drafts and providing feedback. In particular, I would like to thank Professor Subhas Desa, who has been very supportive for both of my undergraduate and graduate life. I have the privilege of working as teaching assistant for Subhas during most of my Ph.D. life, where he has provided me a lot of valuable advice and supports. I would like to thank Professor David Lee who provided advice and assistant in several aspects during the research. I want to acknowledge Professor Olusola A. Ajilore for his support and collaboration. None of the work would have been possible without the support from Olu, who has provided the dataset and has been invaluable sources of knowledge and support.

I further benefited from support from many members of the faculty at UCSC from both TIM and CSE department. Also, I would like to thank members of creative coding lab for all the support and help throughout my research. In particular, I would

like to thank Dr. Manu Mathew Thomas, who assisted in developing several key components in TempoCave described in Chapter 2 and provided advice when developing machine learning model described in Chapter 4. I would also like to thank Dr. Oskar Elek, David Abramov, Hongwei (Henry) Zhou for their advice and supports over the years.

Finally, I owe special thank to my sister, Ning Xu, who has dedicated a lot of time supporting and encouraging me during many sleepless nights.

Chapter 1

Introduction

1.1 Overview

The human brain consists of billions of neurons and trillions of connections. In order to study the activity patterns, researchers proposed using connectome to represent the complex brain network as structural and functional connectivity between brain regions. The term "connectome" was initially suggested by Sporns et al. [62] in 2005 and connectome can be mapped in different levels of scales: microscale, mesoscale, and macroscale. Microscale is at the level of individual neurons and mesoscale is at the level of local circuits that link hundreds or thousands of neurons. Both of them present technical challenges and are avoided in the analysis process. Connectome in macroscale, where neurons are grouped together forming a region, is widely being used for brain studies.

The commonly used technologies for generating connectomes are *diffusion*

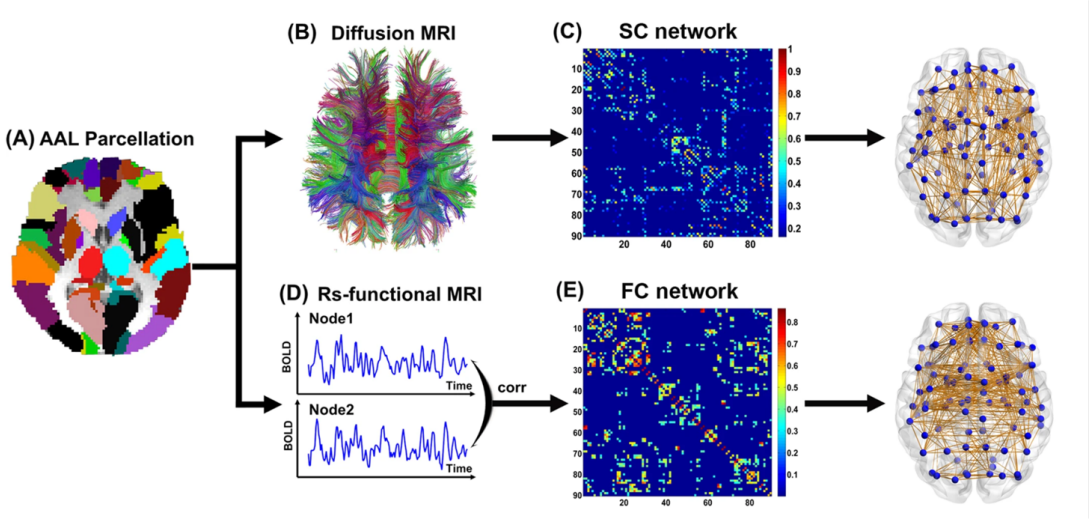

Figure 1.1: The flowchart of structural and functional connectome construction [61].

weighted magnetic resonance imaging (dMRI) and *functional magnetic resonance imaging* (fMRI). dMRI assess the structure connectivity by measuring the white matter structure of the human brain and reconstructing the major fiber bundles in the brain. On the other hand, functional connectivity is statistical correlation between brain region's blood oxygen level dependent (BOLD) signal from fMRI. The statistical correlation often used is Pearson correlation, where the Pearson's correlation coefficient are calculated between pairwise brain regions time series signals. The process of generating structural and functional connectome is usually combing the brain parcellation (different brain regions) with the structural or functional network, as shown in Figure 1.1.

Functional Connectome studies have been widely conducted in clinical studies for finding functional abnormalities of brain disease. Initial studies for functional connectivity (FC) was under the assumption that functional connections during resting

state is static. Static functional connectivity (sFC) has already proven to be significantly related to disease such as depression, schizophrenia, and Alzheimer's disease. For instance, Yan et al. claimed reduced default mode network functional connectivity in depressed patients [76]. Alzheimer's disease patients showed decrease positive correlations between the prefrontal and parietal lobes from the experiments conducted by Wang et al. [67]. Schizophrenia patients experience more diversity of brain functional connectivity [47]. While studies based on static functional connectivities were useful, recent studies show that dynamic functional connectivities (dFC) have hidden correlations for these mental disorders [36, 69, 30].

Common way of getting dFC is from sliding window correlation. As shown in Figure 1.2, on the left, we can see the process of generating static connectivity, where only one correlation matrix is calculated for the whole time series fMRI scan. On the right of the figure, we see the process of getting dynamic connectivity by sliding window correlation, where one correlation matrix is from a small time window, and after sliding the window by some distance, next correlation matrix of next time window is generated. Thus dynamic functional connectivity contains time series of correlation matrix [5].

Allen et al. had developed an approach for analyzing dynamic functional connectomes based on independent component analysis, sliding time window correlation, and k-means clustering of windowed correlation matrices [5]. They cluster connectivity dynamics into different states and based on the identifies states, they analyze a variety of parameters such as mean dwell times, transition probabilities, and graph theoretic measures that describe the observed FC patterns and brain dynamics. This has provided

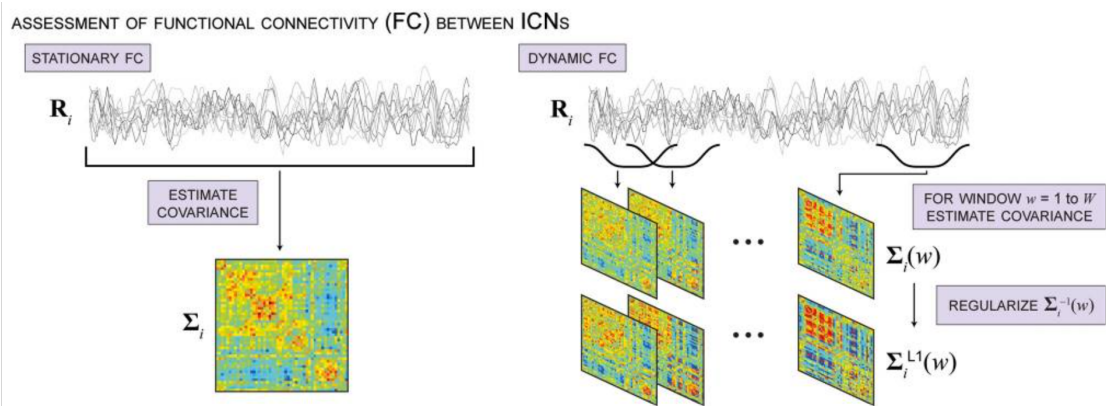

Figure 1.2: Static Functional Connectivity (sFC) matrix generation using statistical correlation (left) and dynamic Functional Connectivity (dFC) matrix generation using sliding window correlation (right) [5].

the foundation for the analysis of dynamic functional connectomes and is commonly used. Even though the clustering method explain the data well without predefined biological assumptions, they are not able to provide detailed information about brain region temporal connection patterns. Current assumption based approach is limited to certain brain regions, and the result might differ based on different dataset, which means the current research based on predefined hypotheses from prior static research and test the dynamic of functional connections of certain brain regions.

The existing analysis tool includes graph theory for identifying the connectivity patterns of human brain networks. To find patterns in high dimensional data, machine learning technique such as SVMs and neural network are utilized. Although Convolution Neural Network (CNN) shows promise in extracting features from images, it doesn't perform well with unstructured data such as brain networks. Graph Neural Network

are well suited for processing connectome data. However most tools are limited in extracting features from static connectome and ignore temporal features. There does not exist a data driven method for deriving and verifying hypotheses for the entire dynamic connectome.

Important features of connectomes include: structural information (brain region anatomical information), connectivity between regions, and brain regions modularity classifications. For brain regions, other than anatomical information, neuroscientist usually classify brain regions into different modules defined by their functional roles in cognition. Both connectivity between brain regions and their modular affiliation vary over time in functional connectomes. Due to the high density of regions and connections between them, neuroscientists have been relying on visual analysis tools. Understanding the structure and functionality of connectomes through visualization is important for getting insights of the behavior of various brain conditions.

Several visualization techniques have been proposed to assist neuroscientists in their analysis. The most basic visualization for representing the voxel functional connectivity is a two dimensional matrix, such as Fig. 1.3a. Such visualization can't encode anatomical information. Bullmore et al. [12] suggested using graph theory approach to visualize the human brain, where the nodes represent brain regions, and edges represent the gray matter morphological correlation or white matter fiber connections in structural connectome or temporal correlation in functional connectome. Many visualization techniques and toolkits exist for extracting brain network topological and connectivity properties, including *Connectogram* [35], *BrainNet Viewer* [72], *eConnec-*

tome [31] shown in Fig. 1.3b, 1.3d, 1.3c. These visualizations focus on either static or 2D representation, which lacks spatial information or dynamic features of Connectome. To our best knowledge, there is only one visualization implementation, *BrainX*^{3} [6], to visualize a single 3D dynamic connectome but is limited to a single connectome with no comparative analysis. Visualizing multiple dynamic connectome in 3D representation is a challenging problem and needs further investigation.

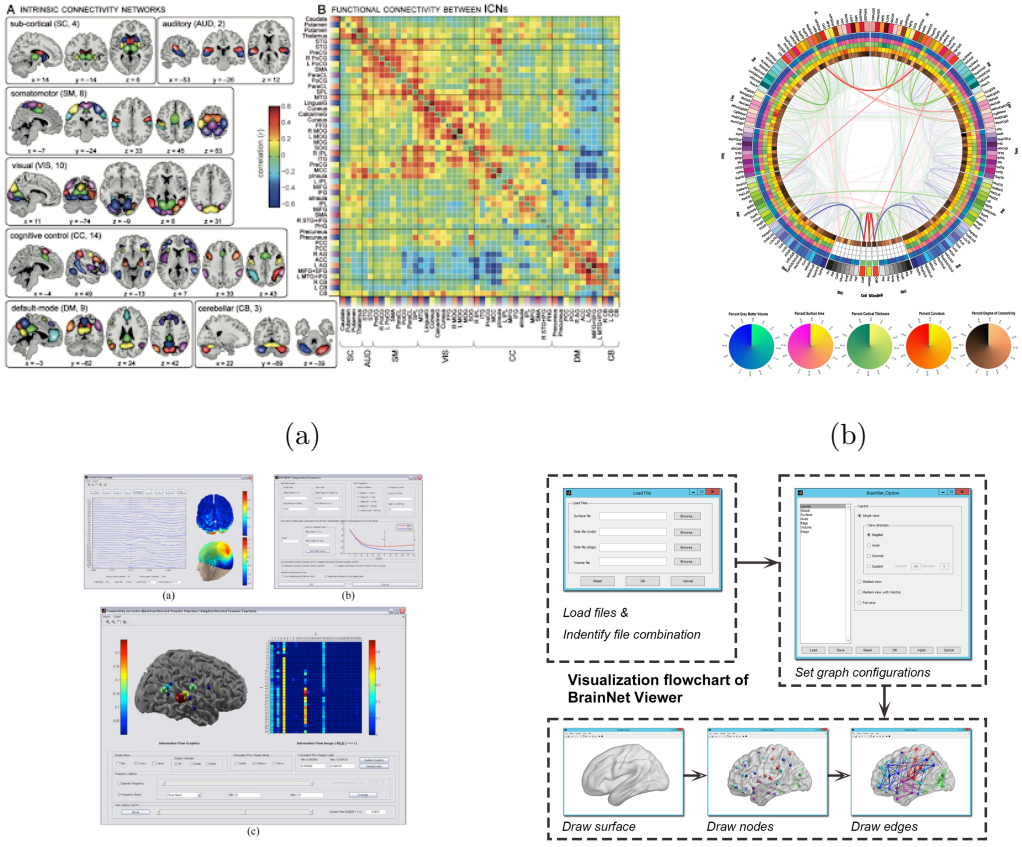

Figure 1.3: Existing Connectome Visualizations: a Allen et al. 2012; b Connectomegram Irimia et al. 2012; c eConnectome He et al. 2011; d BrainNetViewer Xia et al. 2013.

We have been working closely with clinical neuroscientists in the Department of Psychiatry, University of Illinois at Chicago. Apart from visually inspecting dynamic connectomes, an important feature they emphasize is comparison of different dynamic networks. One aspect of their work with connectome involves studying the patterns in activity of certain brain regions. Differences in such patterns stand out when comparing connectomes of patients and control groups. Another aspect is identifying the effectiveness of certain cognitive psychotherapy treatments that involve comparing the same patient's pretreatment vs post-treatment connectomes, or patient vs control group connectomes.

1.2 Research Issues

In order to analyze entire dynamic connectomes, we explore research in areas of data visualization and machine learning, which will benefit clinical neuroscience. The following research issues explored in this thesis relate to visualization, machine learning and neuroscience.

- **Research Issue 1: Visualization Research** Visualizing densely interconnected networks is one of the most challenging aspects of data visualization. As mentioned previously, neuroscientists rely on visual analysis and comparing different connectomes are very important. However, very little research has been done to address comparing dynamic interconnected networks. In order to preserve the spatial relationship of brain regions and connections, we want to visually com-

pare connectomes in 3D representation, as well as observing dynamic connections and modular affiliations. We address this issue by exploring different visual encodings and developing visualization applications with collaboration with clinical neuroscientists. The details for the applications are described in Chapter 2 and 3.

- **Research Issue 2: Machine Learning Research** Visualization tools can help researchers observing dynamic networks, however, the complexity of connections increases exponentially when number of brain region increases. It is important to highlight the important differences between two or more multiple dynamic networks. However, there does not exist a data driven method for analyzing based on comparing entire dynamic connectomes.

  In order to find patterns and get feature representation of comparing high dimensional dynamic connectomes, we explored machine learning classification model to analyze. Machine learning techniques have proved to be able to classify two groups of brain networks, but most of the work is limited to static functional connectomes. Graph neural networks are a promising recent approach to discovering meaningful patterns in connected network data. Current GNN models are not suitable for temporal networks. In this thesis, we address this issue by modifying the model of GNNs that enable their application to time-series network datasets. A detailed description of the novel GNN model is provided in Chapter 4.

- **Research Issue 3: Neuroscience Research** Even though the machine learning model can provide feature representations for analyzing dynamic connectome

data, it is crucial for neuroscientist to understand the results. Explainability of machine learning models is an ongoing research topic. After analyzing temporal brain networks using machine learning, it is important to determine the how the model makes decisions. To address this issue, we developed an explainable mask mechanism, explained in Chapter 4.

1.3 Our Pipeline

In order to address these issues, we need to combine the visualization and machine learning analysis components in order to provide comprehensive solution. In this work, we develop visualization tools and extend graph neural network to extract temporal features from a dynamic connectome. In addition, we introduce a explainable mechanism combined with interactive visualization tools to understand the learned features. In summary, we propose a novel data analysis and visualization pipeline for dynamic functional connectivity studies. Our pipeline consists of:

- Two interactive visualization tools, *TempoCave* and *ConnectoVis*, that can load multiple dynamic connectomes for exploration, comparisons and for verifying the findings from statistical studies. This part of the pipeline addresses research issue 1.

- A machine learning model using a novel temporal graph neural network, for extracting temporal features from dynamic connectomes. The features are used for classifying disease group from healthy control group. This part of the pipeline

addresses research issue 2.

- An explainable tool to understand and verify the decisions made by the model. This tool can be used to find the most significant brain regions related to a disorder. This part of the pipeline addresses research issue 3.

1.3.1 Visualization Applications for dFC Connectome

In Chapter 2, we present *TempoCave*, a visualization application that facilitates exploration, analysis and comparison of time-varying connectomes. Although we focus on connectomes, *TempoCave* is developed as a general-purpose visualization tool for any 3D temporal network data. *TempoCave* introduced a novel 3D overlay comparison of two connectomes. For dynamic connectomes, a playback feature lets the users scan through the timeline to see different network configurations at different time steps. We developed *TempoCave* iteratively, adding relevant visualization features with individual patients' and group average connectomes for a range of disorders such as autism spectrum disorder, anxiety disorder, and major depressive disorder. We show the effectiveness of *TempoCave* with a clinical study on rumination, a mental disorder characterized by repetitively and passively focusing on symptoms of distress and its causes.

Although neuroscientists found *TempoCave* to be useful in their spatial comparison analysis, it had two main limitations with respect to temporal comparison analysis:

- Difficulty in retaining information about a single network while scanning through the timeline. This can cause problems in finding relationships between network configurations at different time steps. For example, if the time interval between two related network configurations is far apart, then the relationship between them will be hidden by the network states in between.

- Since the temporal network data is represented in a linear fashion, the relationships among multiple networks across different time steps are hard to comprehend.

To overcome these limitations, we extend *TempoCave* to a new platform called *ConnectVis*, as described in Chapter 3, a visualization application that supports both spatial and temporal comparative analysis across multiple connectomes. We provide a side by side temporal and spatial view for exploration and analysis. Temporal view summarizes variation of modular affiliation and connectivity over time while the spatial view focuses on the detailed topological structure of multiple connectomes. We present two use cases on real-world data for Rumination and Anxiety studies to illustrate the effectiveness of our system. We conduct interviews with domain experts to evaluate the applicability of our system in mental disorder studies.

ConnectoVis meets all the visualization requirement for our neuroscientist collaborators in the analysis of dynamic connectomes of mental disorder participants. The analysis process is based on heuristics built using statistical algorithms, so they have a rough idea about the regions of interest before looking at the visualization tools. Using *ConnectoVis* they are able to verify their hypothesis and explore other brain regions.

1.3.2 Temporal Graph Neural Network for dFC connectome

Machine Learning are now widely used for analyzing complex data and extract features or correlations between unstructured data, including neuroscience domain. As mentioned earlier, studies for functional connectivity were mainly focused on static connections, so the application of machine learning for FC are also mainly focused on static connectomes. SVM is the most commonly used model for connectome studies, however it is not suitable for analyzing timeseries data. Connectomes can be considered as graphs, where nodes represent brain regions and edges represent the connections between brain regions. dFC can be considered as dynamic graphs with one connectivity graph at each time frame.

Graph Neural Networks (GNN) is a deep learning technique that designed for graph network data and is now widely used in many domains such as transportation, social networks. Chapter 4, we introduce a novel temporal GNN model that is specifically for dFC connectomes. Our model learns the disease connectome dFC features by comparing and classifying disease group and healthy controls. The model then outputs the representation for the two groups dynamic FC features. However, the high dimensional feature representation is difficult to interpret. In order to improve the explainability, we apply a mask generation mechanism to the dFC data and apply it to the pre-trained feature representations. The mask helps us to narrow down the brain regions responsible for the classification. Our model outputs the feature representation for every node. Using distance metrics, we find brain regions that shows similar dynamics. This al-

lows neuroscientists to identify similar brain regions within same connectome as well as compare same brain regions similarity clusters across different connectomes.

1.4 Contribution

In this work, we propose a novel data analysis pipeline for dynamic functional connectivity. We combine machine learning techniques and visualization for clinical neuroscientists for exploring temporal brain connectome data and compare different groups. Our contributions are:

- We develop visualization tools for exploration, comparison and analysis of dynamic brain networks. Our tool helps clinical neuroscientist to form new hypothesis about temporal connectivities in depression patients. Chapter 2 and 3 described detailed applications and their use cases, addressing research issue 1.

- We introduce a novel temporal graph neural network for extracting temporal features from dynamic connectomes, described in Chapter 4. The features are used for classification of healthy vs mental disorder participants or pre vs post treatments. Our network classifies remitted depression group from healthy control group with an accuracy of 98%, described in Section 4.3. The network is also trained to classify pre and post R-CBT treatment connectomes with 88% accuracy. Section 5.2 described the details. This contribution is related to research issue 2.

- Using a mask generator we are able to explain the decisions made by our tem-

poral GNN model. The mask is used to sort the brain regions based on the difference between the two groups. We found that the top discriminative brain region between remitted depression group and healthy control is right anterior supramarginal gyrus. Our findings align closely with the recent depression and R-CBT treatment studies conducted by neuroscientist based on functional connectivity. Section 4.2.2 and 4.4.1 discussed the details of the process of mask development. This contribution is related to research issue 3.

- We identify similar brain regions using a similarity metrics on the node feature representation, enabling neuroscientist to compare similar region within connectome or across multiple connectomes. Section 5.3 demonstrates a use case for using the similarity metrics. This contribution is related to research issue 3.

- The mask generator can also highlight a sub network that shows difference between two connectomes. Using visualization tool, researchers are able to compare the detailed difference, as described in Section 5.1.

Chapter 2

TempoCave: Visualizing Dynamic Connectome Datasets to Support Cognitive Behavioral Therapy

2.1 Introduction

As stated in research issue 1, neuroscientists have been relying on visual analysis tools. Existed tools rarely focus on dynamic brain networks visualizations. We introduce *TempoCave*, a visualization application that facilitates the exploration and analysis of time-series connectome datasets. We worked closely with our neuroscience collaborators to identify aspects of their analysis workflow not yet supported by existing tools, and to determine which tasks are most relevant for making sense of dynamic

connectomes in clinical contexts:

T1: Measuring the *dwelling time* of brain regions, defined as the length of time a region spends in the dominant community.

T2: Measuring the *flexibility* or particular brain regions, defined as the number of times a region changes modular affiliation.

T3: Analyzing the *connectivity* between brain regions that is used to define modular affiliations, including edges that are defined by either a negative or positive correlation between nodes.

T4: Understanding the overall *dynamics*, or "stickiness" of the connectome, in terms of how dwelling, flexibility, and connectivity metrics change over time.

T5: Enabling the *comparison* of multiple dynamic connectomes, for example, comparing a connectome to a group average, or comparing an individual patient's connectome pre- vs. post-treatment.

These tasks have broad relevance to psychiatry, as a wide range of neurological disorders are linked to the disruption of normal brain connectivity. An important overarching goal of clinical neuroscience is to find relationships between brain activity and neurological disorders, which can then be leveraged to make diagnoses, to guide treatment plans, and to better understand the human brain. In this paper, we focus on connectome datasets gathered during a clinical study on *rumination*, a mental disorder characterized by repetitively and passively focusing on symptoms of distress and its causes. The consequences of prolonged rumination include anxiety and depression [11, 42, 66].

Rumination-focused cognitive behavior therapy, or R-CBT, assists individuals in realizing that their rumination about negative experience can be unhelpful, and coaches them on how to shift to a more helpful style of thinking. For example, patients undergoing R-CBT are asked to remember previous positive mental states, such as a time they were completely absorbed in an activity— the opposite of ruminating [41, 68]. R-CBT appears to be effective at supporting emotion regulation in patients suffering from depression. A preliminary study (described in more detail in Sec. 2.4) finds that patients who continued treatment remained in remission after 8 weeks, whereas patients who did not continue treatment had a higher likelihood of relapse. *TempoCave* facilitates insight into how R-CBT (and other clinical interventions) alters brain behavior. In order to conduct these analyses, clinical neuroscientists make detailed measurements of the brain activity of patients and compare the patients' connectomes before treatment and after treatment, and also compare them against baseline healthy connectomes. Visualizing the dynamics of connections within and between brain regions, measured by dwelling time and flexibility, helps clinical psychiatrists examine the "stickiness" of these connections, where comparatively high measurements of stickiness can imply an unhealthy connectome.

To our best knowledge, *TempoCave* is the first application to support comparison tasks for multiple time-series connectome networks in order to better understand rumination. Our contributions include: (a) a delineation of analysis tasks relevant to reasoning about dynamic connectome datasets; (b) the introduction of a new visualization tool to support connectome-based comparison tasks for both static and dynamic

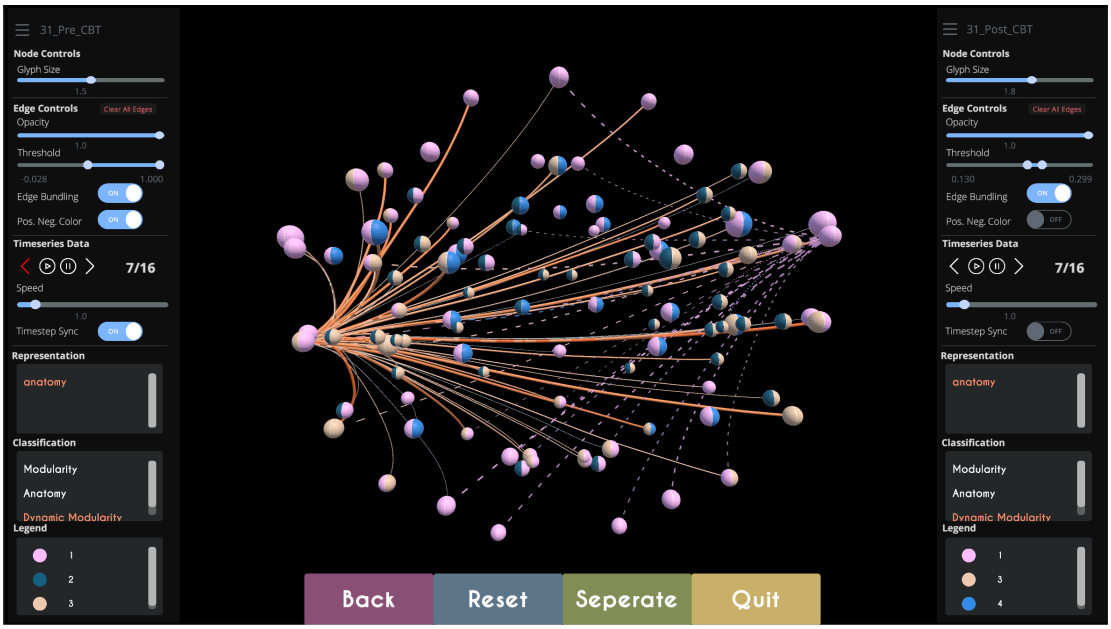

Figure 2.1: A screenshot of the *TempoCave* application. Here, a user compares frames from pre- and post-treatment dynamic connectomes for an individual patient with major depression disorder. Using the option panels on either side of the application, a user can choose different visual encodings to accentuate features useful for understanding the activity of particular brain regions. The left and right coloring of the nodes indicates the modular affinity of a brain region for a patient's pre- and post-treatment connectome, respectively. Likewise, the styling of the connections indicates either the connectome they belong to or the strength of the correlation. A user can synchronize playback of the frames of the connectomes or compare selected frames on demand to gain insight into their dynamics, and during an analysis session a user can interactively toggle on or off brain regions of interest, or switch to alternative representations of the connectome defined using layouts based on dimensionality reduction techniques.

networks; (c) techniques for observing and analyzing community affiliation of nodes in a dynamic network; (d) an analysis pipeline that supports easy data loading of multiple connectomes, including those in alternative topological spaces [78] or generated using different modularity identification algorithms [25, 79]; (e) a real-world use case illustrating how *TempoCave* is used in a clinical setting to elucidate new insight into neurological aspects of rumination. Fig. 2.1 presents an overview of *TempoCave* comparing two dynamic connectomes.

2.2 Related Work

TempoCave is inspired by previous approaches for visualizing networks [10], comparing graphs [29], and exploring connectome datasets [52]. Keiriz et al. [38] survey the landscape of connectome visualization, focusing mainly on static datasets, and characterizing them in terms of their main visualization modality (emphasizing volume, surface, or graph representations), as well as identifying tools that include support for virtual reality (VR) environments. *TempoCave* presents connectomes as 3D networks, similar to approaches presented in *Connectome Visualization Utility* [43], *BrainNet Viewer* [72], *Connectome Viewer Toolkit* [28], and the *AlloBrain* project [63]. However, *TempoCave* specifically focuses on visualizing nodes and edges to make it easier to reason about metrics associated with modular affiliation and connectivity.

TempoCave provides features for dynamic data analysis, presenting a synchronized playback mode that highlights differences between two connectomes at different points

in time. A number of 2D visualizations have been used to explore dynamic connectome data [34, 4, 49, 17], and Beck et al. [10] summarize approaches to visualize 2D dynamic networks. Other tools instead utilize a 3D layout for investigating dynamic connectome data [31, 44, 48]. For example, Xing et al.'s *Thought Chart* [73] presents distinct 3D trajectories for different task conditions and provides a comparative analysis that generates a summary view of how much one dynamic connectome differs in comparison to others. Similar to our implementation, Arsiwalla et al. introduce *BrainX*^{3}[7], an interactive and immersive 3D visualization of dynamic connectomes, but which does not support comparison tasks, a main feature of *TempoCave*.

Alper et al. [3] investigate visual encodings of edge weights within an adjacency matrix to support comparisons of brain connectivity patterns. *TempoCave* further emphasizes comparisons of modularity affiliation metrics that summarize the edge weights in the network. Other recent brain visualization tools focus on neurobiological tasks, such as Ganglberger et al.'s [26] *BrainTrawler*, which provides tools to conduct integrated analyses of genomic data and mesoscale neuroscience datasets at the level of individual neurons. *TempoCave* aims to support tasks **T1**-**T5** relevant to diagnosing and treating patients with neurological disorders, extending previous work that focused on static connectomes [38], which also presents a 3D view and enables a user to explore data immersively [16, 23].

2.3 The *TempoCave* Application

TempoCave is an interactive tool that enables clinical psychiatrists to load, visualize, and analyze dynamic connectomes, solving several technical challenges associated with the analysis tasks described in Sec. 2.1. *TempoCave* supports the investigation of multiple connectomes at once, superimposing connectomes to make comparisons, and providing details about modular affiliation and edge dynamics that are needed in order to understand some dynamic datasets.

Our clinical neuroscience collaborators capture connectome datasets using high-resolution functional magnetic resonance imaging (fMRI) scans. The fMRI data is pre-processed to extract node and edge information, such as connection strength, and to perform various dimensional reduction steps. Dynamic datasets are obtained using scans taken at regular intervals over a short period of time. In the clinical study presented in Sec. 2.4, 200 frames are captured over the course of a $\sim$6 minute scanning session, and then further processed using the PACE algorithm [79] to determine modular affiliations.

TempoCave consists of a selection interface (Fig. 2.2 left), and an interactive inspection interface (Fig. 2.2 middle and right). The selection interface displays show an overview "carousel" of the available connectomes, along with a list of all the available layouts (generated through different dimension reduction algorithms, such as Isomap or t-SNE). The user can select two (in desktop mode) or more (in VR mode) connectomes for analysis and comparison. The inspection interface shows the selected connectomes with each connectome having their own settings panel, which provides options: to change

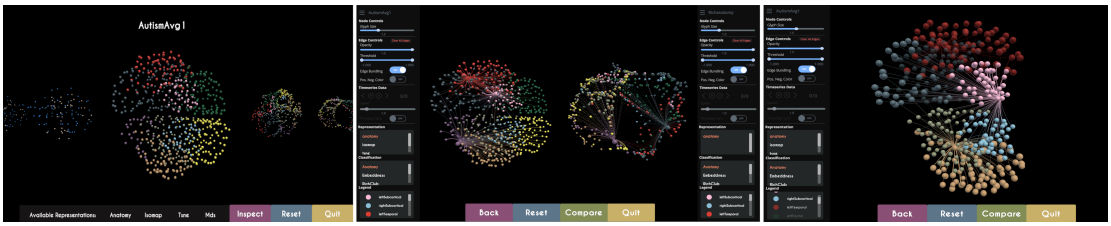

Figure 2.2: Different views in the *TempoCave* interface. Upon starting the application, a thumbnail of all connectomes in the data folder appear in a carousel view (left). Users can add connectomes to the inspection view (middle), which provides a menu panel for each of the selected connectomes and enables users to interactively investigate various connectome features. Users can zoom into a single connectome (right) to more clearly examine the modular affiliation of specific brain regions and to investigate the strength of connections between these regions on demand. In the inspection view, as well as the comparison view shown in Fig. 2.1, a user can also interactively rotate the connectome, toggle edge bundling on or off, change the transparency of edges, increase the size of the nodes, change the visual encodings for nodes and edges, and show or hide selected brain regions or communities. If the connectome has associated alternative layouts, then the user can switch between these views as well, and if the connectome is dynamic, then user can play through the data, or jump to a specified time frame.

the representation of the connectomes, to update the classification of different brain regions, to filter edges based on their connection strength, and to toggle edge bundling to mitigate visual clutter.

Summarizing the modular affiliation or "stickiness" of the nodes in dynamic connectomes is an important aspect of analyzing a patient's connectome, as is investigating the

amount of time that brain regions are associated with particular communities (dwelling time) and the frequency that brain regions change affiliation (flexibility). Connectomes demonstrating patterns of more rapid modular change are believed to indicate healthier connectomes. *TempoCave* automatically processes the summary statistics for each dynamic connectome upon being loaded into the application. For each node in the connectome, changes in the affiliation across the time steps are used to determine the flexibility metric. Dwelling time is calculated by identifying the maximum time a node is associated with a specific module. *TempoCave* uses color-coding to represent both dwelling time and flexibility, supporting **T1** and **T2**. Fig. 2.3 shows how *TempoCave* is used to analyze flexibility in a rumination study.

To analyze changes in dwelling time, flexibility, and edge connectivity over time, *TempoCave* provides controls to scrub through the time steps. Users can play and pause, move forward or backward one or more time steps, adjust the playback speed, and, if two connectomes are available for inspection, there is an option to synchronize the playback settings. At each time step nodes are colored based on their modular affiliation. The edges change their width based on the strength of the connectivity between two nodes, and are colored with a gradient representing the regions they are associated with. The edges can further be classified into positive connections if the regions are correlated or negative connections if they are uncorrelated. *TempoCave* supports an optional color-coding to show the negative and positive edges for each time step, as shown in Fig. 2.1. The dynamic visualization features support tasks **T3** and **T4**. Fig. 2.4 shows an example of how the edge connectivity and modularity change

over time in an analysis session using *TempoCave*.

TempoCave presents an overlay comparison mode supporting **T5**, where two connectomes are juxtaposed to form an integrated layout. Each node in this superimposed view is split into two halves, corresponding to left and right connectomes. As the user moves through the different frames, each half of the node's colors change separately based on the modular affiliation of the associated connectome. The edges can be activated by clicking the corrresponding half of the node. To distinguish the connectivity of two connectomes, we use a solid line for left connectome and a dashed line for the right connectome. A comparison of a pre- vs post-treatment connectome is shown in Fig. 2.1.

We developed *TempoCave* using the Unity Engine, which renders 3D data at real-time frame rates and provides out-of-the-box solutions for immersive applications. We evaluated a range of visual encodings and interaction modalities to determine useful representations and interactions that supported the analysis of dynamic connectomes. For example, we initially included animation as a primary encoding for dynamic network features [57]. While our collaborators found the animation engaging, ultimately it was distracting and introduced visual fatigue when they needed to scrub through many time steps. Instead, we color-coded edges to represent both modular affiliation and edge weights, giving the users the option to choose which encoding was most useful for a particular analysis session. We also experimented with a wide range of shapes to represent brain regions, hoping to more clearly distinguish nodes from different connectomes in the comparison view. However, our users found that it was easier to interpret a

node when rendered as a multi-colored sphere. Contrary to expectations, we discovered that our users preferred to have fewer available encodings overall, but more options to control which data elements these encodings represent.

2.4 Use Case: Investigating R-CBT Treatment

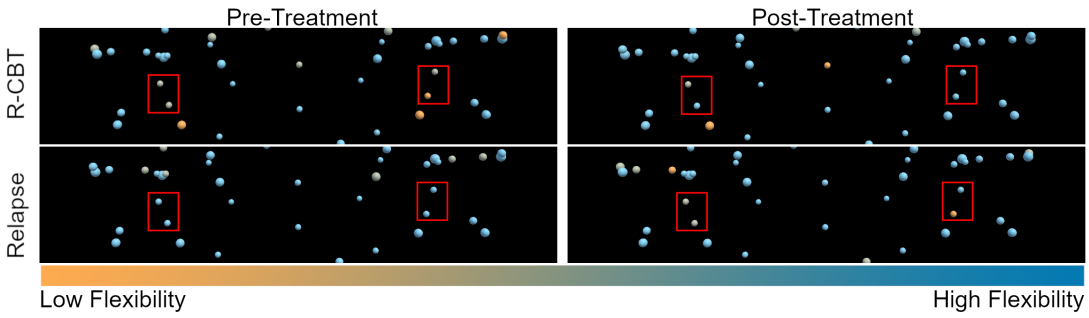

Figure 2.3: This figure shows a summary view of the *flexibility* of brain regions associated with rumination (**T2**). The top images show the connectome of a MDD patient who received R-CBT treatment, indicating higher flexibility (blue nodes) post-treatment than pre-treatment (where the orange nodes indicate lower flexibility). The bottom images show a relapsed patient who did not receive R-CBT, where there is substantially decreased flexibility in brain regions associated with rumination. The red rectangle highlights the two relevant brain regions: supramarginal gyrus (top) and angular gyrus (bottom).

As an initial validation of *TempoCave*, we explored a dataset from an ongoing clinical study that measures the effectiveness of rumination cognitive behavioral therapy (R-CBT) for adolescent patients with at least one previous episode of major depression

disorder (MDD) [13]. In this study, 27 patients were recruited for comparing 8 weeks of R-CBT data against a control group of 15 healthy participants. The patients were in remission at the start of the study, and the main goal of the study was to measure the effectiveness of R-CBT at preventing a relapse of depression. Of the 27 patients with MDD, 14 were administered a treatment of R-CBT, and none had a relapse during that time. Of the 13 who were not administered R-CBT, 4 patients had an episode of MDD, providing initial evidence of the efficacy of R-CBT. Using *TempoCave*, clinical

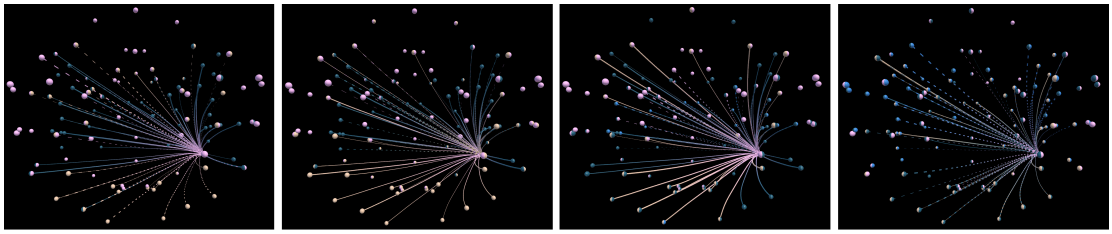

Figure 2.4: This figure presents the dynamic connectome of a patient with MDD who received R-CBT. Here, the overlay comparison reveals differences in modular affiliation and in connectivity patterns pre- vs. post-treatment across multiple time steps.

psychiatrists observed the modularity dynamics of individuals' connectomes. Participants from a healthy control group were found to have a higher overall flexibility than patients with MDD, and that on average there is no significant difference between the pre- and post-treatment connectomes of MDD patients who received R-CBT. However, as depicted in Fig. 2.3, the post-treatment connectome of MDD patients who did *not* receive R-CBT (and relapsed) shows much less flexibility than was observed in their pre-treatment connectome. Fig. 2.3 highlights the supramarginal gyrus and angular

gyrus, two regions that are indicated in depression disorder. Fig. 2.4 shows an overlay comparison view of a patient's pre- and post-treatment connectomes who received R-CBT, where the angular gyrus is selected. Looking at the right half of the selected node (from the post-treatment connectome), clinical psychiatrists found that the angular gyrus changed modularity three times (from t=2 to t=14), but that in left half of the selected node (from the pre-treatment connectome) the modularity of angular gyrus changed only once (from t=8 to t=14). This visual analysis corroborates the hypothesis that R-CBT mitigates rumination, as indicated by the temporal dynamics of dwelling time and flexibility metrics.

2.5 Conclusion & Future Work

Our initial use case already indicates that *TempoCave* helps clinical neuroscientists form new hypotheses about dynamic connectome datasets, and in particular that the comparison mode is useful for providing insight into patterns that emerge when investigating a patient's response to treatment. Future work will explore a wider range of use cases in various clinical contexts. Additional definitions of modularity could generate network metrics that may be useful for understanding brain dynamics. For instance, recent work by Kim and Lee [39] introduce an inconsistency metric which can be used as an alternative definition of node centrality. Furthermore, while *TempoCave* provides textual labelling of nodes and edges, our collaborators indicated the need for including additional annotation options, which would make it easier to share

results or hypotheses with other clinicians and to include as figures in presentations and articles. We also plan to extend our approach to other (non-connectome) dynamic datasets, and to conduct user studies to determine the effectiveness of our visual encodings as a more general approach for highlighting dynamic network features and comparing networks. *TempoCave* is available via our open source GitHub code repository at `https://github.com/CreativeCodingLab/TempoCave`, along with source code, detailed instructions on how to load in custom datasets, and additional documentation.

Chapter 3

ConnectoVis: Spatio-Temporal Exploration of Dynamic Connectomes

3.1 Introduction

The structural and functional connectivity mapping of the human brain allows neuroscientists to acquire a deeper understanding of various brain conditions [62]. Maps of these neurological connections are known as connectomes and are obtained by processing functional magnetic resonance imaging (fMRI) scans of the brain. Connectome datasets consist of nodes that represent brain regions and edges that represent the strength of the connectivity between these regions. Additionally, each node can be assigned a modular affiliation associated with a particular brain function, which can vary over time in response to different tasks. The exploration and analysis of connectomes is challenging in part due to the large amount of data, and the complexity of the

data increases with temporal connectomes, created from fMRI captures taken in quick succession. Many visualization techniques exist for exploring brain networks, such as *Connectogram* [35], *Connectome Visualization Utility* [43], *BrainNet Viewer* [72], *Connectome Viewer Toolkit* [28], and *NeuroCave* [38]. However, these tools focus on static networks and do not facilitate the exploration or analysis of dynamic connectomes.

Furthermore, in psychopathological studies, making comparisons between healthy control groups and patients plays a key role in gaining insight into mental disorders, such as Alzheimer's disease, schizophrenia, epilepsy, and major depressive disorder (MDD). For instance, Ma et al. [51] examined dysfunctions in brain regions across patients with schizophrenia, bipolar disorder (BD), and MDD by comparing 121 schizophrenia, 100 BD and 108 MDD patients with 183 healthy controls. Liao et al. [45] conducted a study where they found that modular structures of brain networks vary across individuals by comparing temporal variation of modular affiliation. Burkhouse et al. [13] studied the abnormal activity in regions within the DMN and in areas involved in visual, somatosensory, and emotion processing of remission from MDD patients using comparative analysis. Xing et al. [74] studied the connectome features of social anxiety disorders by comparing 20 healthy controls and 20 anxiety participants' temporal connectomes. In each of these studies, researchers compare different connectomes on either an individual level or group average level in order to understand brain behavior under particular diseases. Important features for comparison include both the modular affiliation associated with and connectivity between brain regions as they change over time. As articulated by Pfister et al. [55], it remains a challenge to design comparative

visualizations of dynamic networks without losing spatial and temporal information.

To the best of our knowledge, no existing tool provides dedicated support for spatio-temporal comparison of multiple connectomes. We introduce *ConnectoVis*, a visualization tool that supports the analysis of dynamic connectomes. *ConnectoVis* includes synchronized views enabling users to more effectively examine features of connectome datasets, such as identifying similar modularity and connectivity patterns within the same connectome or across multiple connectomes. Our temporal view summarizes variation in modular affiliation over time, while our spatial view focuses on the connectivity patterns within the topological structure. Our tool supports the selection of multiple connectomes, subnetworks, and brain regions, visually highlighting both positive and negative connectivity between them [79]. To illustrate the effectiveness of *ConnectoVis*, we present use cases exploring clinical datasets for studies on *rumination*, a mental disorder characterized by the persistent replaying of negative thoughts. A screen capture that shows an overview of *ConnectoVis* is shown in Fig. 3.1.

Our previous work: *TempoCave* is a tool that provides a 3D overlay comparison of two temporal brain networks. Clinical neuroscientists found *TempoCave* useful for analyzing connectomes, however our collaborators later expressed a need for tools to support additional analysis tasks. For example, *TempoCave* provides a playback feature, but it can be difficult to retain contextual information while scanning through the time steps, especially as the time interval between two related network configurations increases. Moreover, it became apparent that it is important to provide a visual overview of temporal statistics related to modular affiliation, which helps researchers to identify

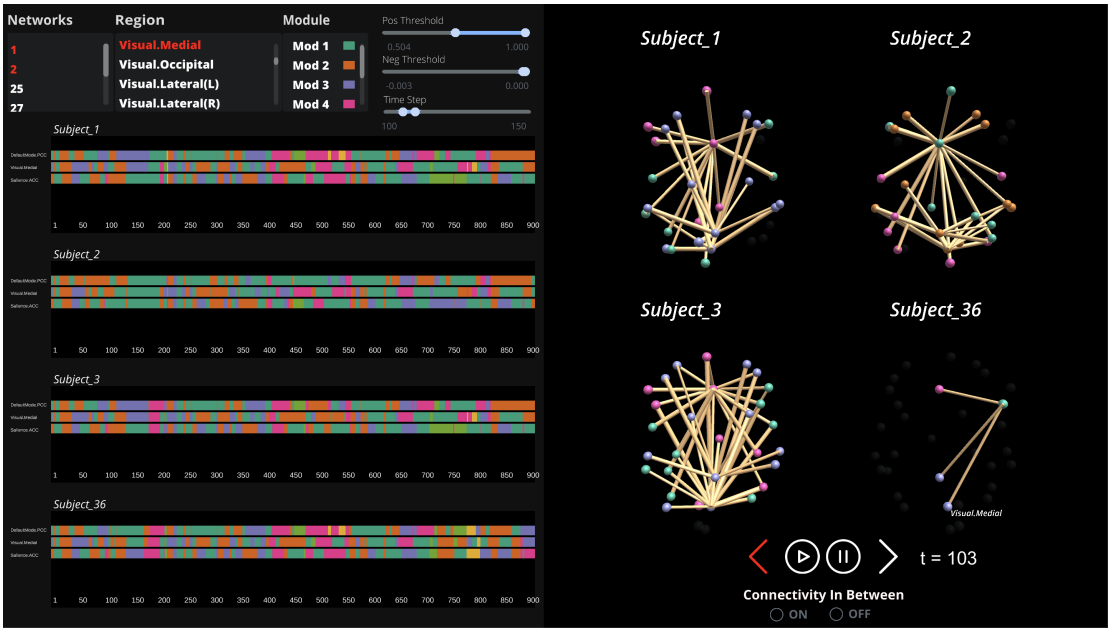

Figure 3.1: Overview of the *ConnectoVis* software tool. The *temporal* view (left) currently shows the modular affiliation changes for three regions per connectome. The 3D *spatial* view (right) shows the detailed topological information related to these regions for each of the four currently selected connectomes. Connectivity patterns and modularity dynamics can be interactively investigated and compared by selecting one or more nodes on the spatial view, or via the control panel. Connection strength and time range filters enable nuanced exploration of the connectomes, and a playback feature supports temporal navigation.

potentially interesting patterns that can then be explored in more detail via a network representation. Furthermore, the primary visual encoding in *TempoCave* juxtaposes two networks with similar topological configurations, which makes it difficult, for example, to analyze data from connectome studies involving multiple participants [13, 51]. Similarly, task-based anxiety studies may require the simultaneous comparison of patients' brain dynamics across different tasks [74].

We developed a list of primary analysis tasks based both on this feedback and through interviews with clinical neuroscientists from two different labs (University of Illinois at Chicago's Computational Neuroimaging and Connected Technologies Lab and Beijing Normal University's Institute for Brain Research) who perform dynamic connectome analysis as part of their research. We summarize the main tasks supported by *ConnectoVis* as follows:

T1: *Comparing multiple dynamic connectomes.* Clinical neuroscientists may make comparisons between a single patient's pre-treatment and post-treatment connectomes, a group average of patients with a particular disease and healthy controls, two patients with a similar neurological issue who received different treatments, or connectomes from the same patient but responding to different tasks.

T2: *Identifying temporal patterns based on modular affiliation.* Researchers need to understand at-a-glance when modular affiliation changes rapidly across particular brain regions, which could indicate a particular disorder.

T3: *Visualizing topological structures in 3D space with respect to individual time-steps.*

Researchers are interested in understanding the dynamics of connectivity patterns at particular time steps where there are changes in modular affiliation.

T4: *Filtering data to focus on regions of interest.* Clinical neuroscientists are often interested in the activity of particular brain regions within particular time slices and above or below thresholds of connectivity strength, and need to be able to select subnetworks made up of nodes known to be associated with a particular disease.

Key to supporting these tasks is facilitating the ability to move between summary views and more detailed comparison views in order to understand the temporal dynamics of connectivity patterns and modular affiliation patterns within selected brain regions. Additionally, our neuroscientist collaborators noted the importance of interacting with multiple connectome datasets with high spatial and temporal resolutions in real-time. Below, we describe the main features of *ConnectoVis*, a visualization tool that supports **T1**-**T4**, incorporating both a 2D temporal view and a 3D spatial view to enable the exploration of the temporal dynamics of multiple connectomes.

3.2 Related Works

Recent projects present visualization tools for investigating connectome datasets [2, 26, 48, 50, 38, 73, 16], some of which focus specifically on enabling graph comparison tasks [70, 58]. For example, Yang et al. [77] propose a hybrid representation to support blockwise brain network visual comparison, and Fujiwara et al. [24] introduce a visual analytics system to compare brain connectivity between individuals and groups.

ConnectoVis also supports comparative analysis, enabling the comparison of multiple dynamic connectomes.

Geniesse et al. developed dynamic brain neuroimaging data visualization by dimensional reduction which studies the relationship between each time frames. The approach didn't consider the connectivities features between brain regions, and it's also hard to do comparison. [27]. In order to represent large time series datasets, *Time Curves* [9] provides a approach for visualizing temporal dynamics, utilizing a dimensionality reduction step to embed time points in 2D space. For connectome datasets, it can be easier, and more familiar for our clinical neuroscientist users, to explore connectivity patterns via a 3D network representation. *ConnectoVis* displays multiple dynamic networks along with a temporal overview summarizing modular affiliation for selected nodes.

A range of works, including *GraphDiaries* [8], *DMNEVis* [54], *TempoVis* [1], describe techniques involving combined timeline and network views. *ConnectoVis* also features a timeline view to provide temporal context for brain connectivity patterns. Similar to other projects that feature multiple brain network representations side-by-side [21, 24, 49], the *ConnectoVis* layout makes it easy to integrate different perspectives of the data, facilitating a richer analysis of connectome dynamics.

3.3 The *ConnectoVis* Application

As illustrated in Fig. 3.1, *ConnectoVis* consists of two views and associated control panels, a *temporal* view and a *spatial* view. The temporal view displays changes in

modular affiliation over time for user-selected brain regions on a 2D timeline. The spatial view provides an interactive network layout showing the 3D topological structure of user-selected connectomes. These two views are synchronized, and selecting or filtering the data in one view updates the data in the other. Together, these two views provide insight into the spatio-temporal dynamics of in connectome datasets. *ConnectoVis* includes a control panel to load in datasets and to select particular connectomes and brain regions of interest. It also includes range sliders to filter positive and negative connections above or below particular thresholds, or to focus on particular time ranges. Additionally, a playback feature lets users navigate the network representation across time. *ConnectoVis* enables neuroscientists to upload any number of static and dynamic connectomes. (A static connectome is treated as a connectome with a single time-step.) In addition to anatomical representations of brain networks, *ConnectoVis* supports 2D or 3D representations resulting from various dimensionality reduction techniques, such MDS, t-SNE and Isomap [78]. Once the connectomes are loaded, using the list view, users can select multiple connectomes and multiple brain regions for comparative analysis. Moving between the synchronized temporal view and spatial view facilitates identification of modularity affiliation patterns over time and the corresponding connectivity patterns for particular brain regions. By showing information for multiple connectomes simultaneously, neuroscientists can quickly compare different brain regions, either within the same connectome, or between different connectomes, supporting task **T1**.

The temporal view consists of a timeline for each selected connectome, highlighting dynamics in modular affiliation, as shown in Fig. 3.1 (left). By default, we limit the

selection to 5 brain regions per connectome to avoid visual clutter. When a region or a node is selected from the control panel or from the spatial view, the modular affiliation of the selected region is shown as a color encoded horizontal bar graph across the currently selected range of time steps, supporting task **T2**. Color is mapped to module, indicating which module the selected node is associated with at each time step.

The spatial view displays selected connectomes in a 3D node-link representation. Each node or region is encoded as a sphere with a spatial location, by default mapped to anatomical position. The nodes are shaded based on modular affiliation, matching the colors used in the temporal view. The edges between nodes are represented using 3D cylinders, and their thickness indicates connection strength, supporting task **T3**. By default, the spatial view displays four 3D network structures simultaneously, with individual support for zoom, pan, and rotation. Users can select one or more regions from any of the node-link diagrams, which immediately updates the display in the temporal view. To reduce visual clutter, deselected regions are faded out, but still slightly visible to provide spatial context. Users can adjust the time range slider to focus on time steps with interesting connectivity patterns. Further, users can also select an option to only show the connections between currently selected brain regions, hiding all other edges in the network. Some connectome datasets define both a positive and negative connectivity strength, and in some situations, users may want to focus only on strong connections above a particular threshold, and two sliders are provided to support filtering on positive or negative connectivity. The controls and visual encodings provided for the spatial view support task **T4**. The spatial view is shown in the Fig. 3.1

(right).

Here, we outline a typical *ConnectoVis* workflow. First, after loading the connectome dataset, users can select up to four individual connectomes from the list view to be examined at the same time. These connectomes' 3D network representation will be displayed in the spatial view. A user can then select nodes of interest (mapped to particular brain regions) either from the spatial view, by clicking on the nodes in the network, or from the temporal view, by clicking on the names of brain regions listed in the control panel. The connectivity of the selected brain region is shown in the spatial view, and the modular affiliations of the selected brain region will be displayed in the temporal view. For instance, in many studies exploring major depression disorder, neuroscientists are interested in examining the angular gyrus (AG) brain region, as it is known to be an indicator of unhealthy brain activity. Upon selecting a node representing AG in the spatial view, a summary of AG modular affiliation over time for the currently selected time range is added to each connectome in the temporal view, and the connectivities from AG to other regions are shown for every connectome in the spatial view. In the temporal view, a neuroscientist can get an at-a-glance overview of the "stickiness" of AG modularity, and can quickly identifying interesting time ranges where modular affiliation changes rapidly. The neuroscientist can then examine the spatial view for more details about the connectivity and modularity of the brain regions that are directly connected to AG. Mental disorder studies often involve examination of multiple brain regions. Using *ConnectoVis*, neuroscientists can iteratively select regions related to AG for further examination, such as the posterior cingulate cortex (PCC)

brain region. The modular affiliation of PCC will then be displayed below AG in the temporal view, supporting temporal comparison between brain regions within the same connectome or across mmultiple connectomes.

ConnectoVis is designed to render multiple connectomes simultaneously with high spatial and temporal resolution in real-time. *ConnectoVis* was developed using Unity Engine v2018.3, enabling us to render different views of multiple dynamic connectome at real time rates on 4K displays, including the 3D spatial view and the 2D temporal view. Each dynamic connectome datasets can typically be between 1-20 MBs in size, depending on the number of time steps and the resolution of the fMRI scans. Connectome datasets are comprised of various CSV files, and normally include connectivity and modularity matrices for every time step, along with the spatial coordinates for each node. In addition to standard anatomical layouts, some connectome datasets also provide alternative topological representations resulting from processing the data using dimensionality reduction algorithms. *ConnectoVis* pre-loads all the connectome datasets, and we use geometric instancing to reduce the render call for identical mesh data and level-of-details (LOD) to reduce the mesh resolution for regions not in focus. (We have used *ConnectoVis* to display 9 high resolution connectomes simultaneously at real time rates, but our neuroscientist collaborators suggested that a default of 4 is sufficient for comparative analysis and helps to to reduce visual clutter.)

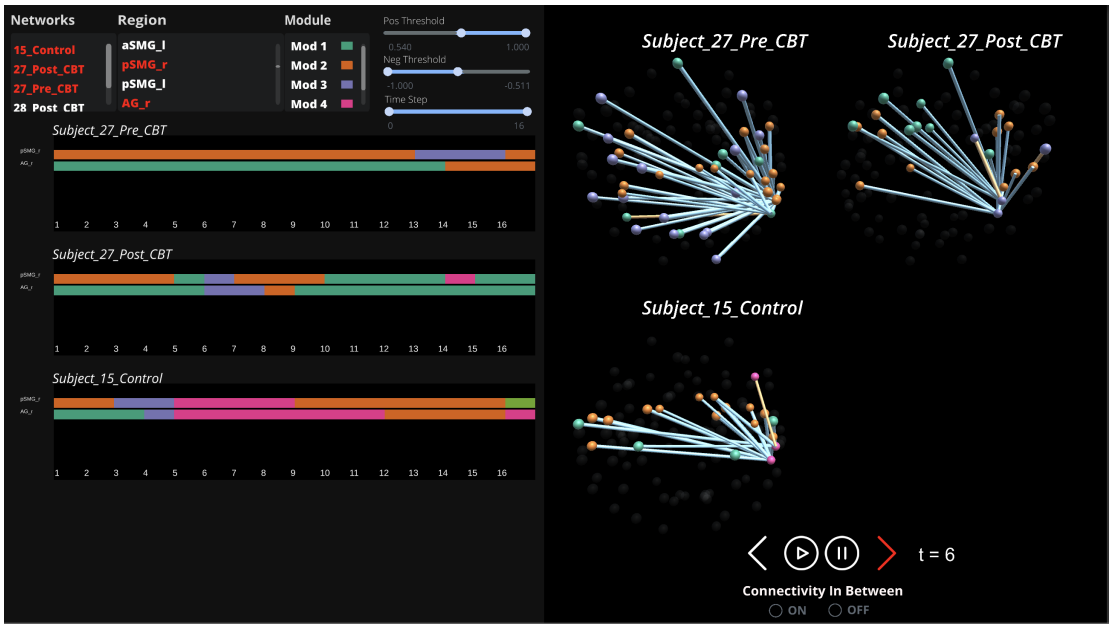

Figure 3.2: *ConnectoVis* displaying selected connectomes from the rumination relapse study. Top two connectomes in the temporal and spatial view represent subject #27 pre and post R-CBT treatment. After receiving R-CBT, subject #27 shows improved flexibility in brain region right angular gyrus and right posterior supramarginal gyrus, compared to pre-treatment, as indicated by the modular affiliation dynamics. A connectome from the control group (control #15) is also selected for reference.

3.4 Use Cases

Working with our neuroscientist collaborators, we evaluated *ConnectoVis* by analyzing connectome datasets derived from fMRI scans to investigate the relationship between rumination and major depression disorder (MDD).

First, we ran *ConnectoVis* using a dataset from a clinical study on "rumination relapse". The dataset consists of temporal connectomes derived from fMRI images, and

then processed using PACE algorithm to detect modular affiliation [79]. The clinical study had 42 participants, 27 of who were diagnosed with rumination, 15 of them are healthy controls. Of the 27 rumination patients, 14 received rumination-focused cognitive behavior therapy (R-CBT) treatment during an 8 week period, and none had a relapse during that time. Of the 13 who were not administered R-CBT, 4 patients had an episode of MDD, providing initial evidence of the efficacy of R-CBT to prevent relapse. Using *ConnectoVis* to investigate temporal features across the time range for multiple brain regions helped neuroscientists reason about changes in modular affiliation and to hypothesize about whether the "stickiness" of certain brain regions is a factor in MDD. Fig. 3.2 shows data for three selected dynamic connectomes from this study. Here the pre- and post- treatment connectome for subject #27 is being investigated, with a healthy control #15 shown for comparison. Two regions, the right posterior supramarginal gyrus (pSMG_r) and the right angular gyrus (AG_r), are thought to be indicated in rumination disorders, and are visible in the temporal view (Fig. 3.2, left). We can see that pSMG_r in the pre-treatment connectome for subject #27 is associated with a single module (orange) from T1 through T12. However this subject's post-treatment connectome shows modularity shifts 4 times on the same region during the same length of time. The AG_r region shows a similar pattern. This provides initial evidence that after receiving R-CBT treatment for a 8 week period, subject #27's tendency toward rumination has decreased. Researchers can also load in additional connectomes to make sense of temporal patterns. Here, control #15 is used as a benchmark to compare subject #27 to a healthy patient. Using the threshold sliders to highlight

strong connections, researchers can identify more subtle differences between the brain activity in healthy and depressed patients, as shown in the spatial view (Fig. 3.2, right).

Second, we ran *ConnectoVis* using an open source dataset available from the Nathan Kline Institute (NKI) [53] containing 32 nodes and 900 time steps (see Fig. 3.3) in order to investigate the relationship between temporal dynamics and Ruminative Responses Scale (RRS) scores [64], where higher RRS scores indicates that a patient is more likely to suffer from depression and to engage in rumination. From this dataset, our neuroscientist collaborator collected 68 subjects showing evidence of rumination. Previous analysis indicates that the right lateral parietal (LP_r) is significantly correlated with rumination [13], and *ConnectoVis* was used to interactively explore modular affiliation and connectivity dynamics in the LP_r region for these subjects. Fig. 3.3 shows an example from this analysis session, with subjects #1, #25, #27, and #42 currently selected. Their associated RRS scores are listed in Table 3.1. We can see that subject #25, whose RRS score is relatively low, shows higher flexibility in the LP_r region, especially during time range 700 through 800. The other subjects, with higher RRS scores, show less flexibility in this region, especially during this time range. As shown in the spatial view, subject #25 also demonstrates weaker connectivity from LP_r to other brain regions than the other subjects do. That is, *ConnectoVis* provides initial validation for the hypothesis that the RRS score is positively correlated with increased overall connectivity in the LP_r region.

These analysis sessions demonstrate that *ConnectoVis* is effective in supporting tasks **T1**-**T4** to explore temporal patterns in connectome datasets, and that it is a useful

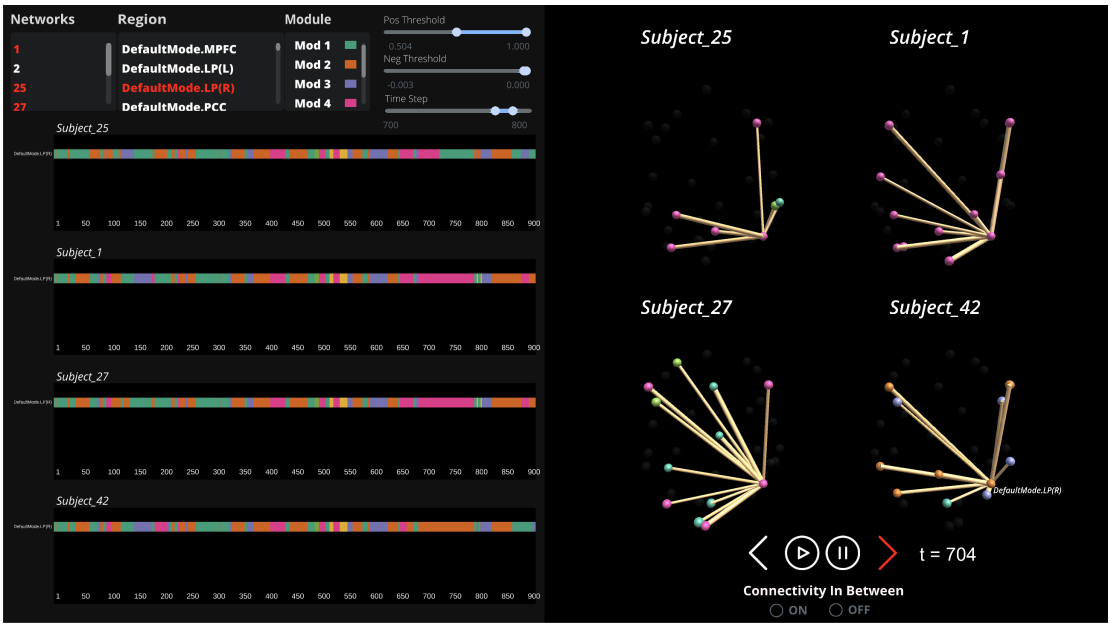

Figure 3.3: *ConnectoVis* displaying selected connectomes from the Nathan Kline Institute's rumination dataset. Here, we can see that subject #25 (with a lower RRS score) shows more flexibility in modularity dynamics and weaker overall connectivity than the other three subjects in the right lateral parietal brain region, indicating that the brain region is positively correlated with rumination.

tool for researchers comparing pre- vs post-treatment connectomes in a single subject, comparing individual subjects across different tasks, and for comparing multiple subjects with the same disorder.

3.5 Conclusion and Future Work

We presented *ConnectoVis*, a novel visualization tool for the spatio-temporal comparison of multiple dynamic networks. Our tool focuses on identifying changes in modular

Subject	RRS Depression Score (Max 48)	RRS Brooding Score (Max 20)	RRS Rumination Score (Max 20)	RRS Total Score (Max 88)
1	24	8	12	44
25	13	8	5	26
27	44	18	12	74
42	45	18	14	77

Table 3.1: Ruminative Responses Scale (RRS) scores [64] for selected subjects from the NKI datasets. The higher score suggests more depressive, brooding, or ruminative behavior.

affiliation and connectivity patterns using integrated temporal and spatial views, and was useful for investigating rumination in connectome datasets. In addition the use cases presented above, we gathered expert feedback on *ConnectoVis* from neuroscientists at two different labs, each of who appreciated the summary view of subjects' brain activity made available in the temporal view. They also found the coordinated views to be useful, with one neuroscientist telling us that it made it easier to identify the brain regions of subjects that were mainly affiliated with a particular module, and that the temporal view was a good starting place for exploration before investigating connectivity patterns in the spatial view, which is necessary for comparing, for example, differences in pre- vs. post-treatment for different subjects. Clinical neuroscientists analyze their data by performing various statistical methods on the connectome datasets. However, due to the sheer amount of data, it can become tedious to examine the activity in particular brain region manually, especially for dynamic networks. Using our

tool, they can interactively select the region of interest and investigate and compare the activity within or between connectomes, greatly speeding up their investigation of the data. Moreover, one neuroscientist noted that a limitation to their statistical approach is that it is performed on nodal averages or time range averages, which can obscure the detailed modularity and connectivity dynamics of an specific regions. *ConnectoVis* introduces useful features that enable neuroscientists to find and examine nodes with similar modularity and connectivity patterns within the same connectome or across multiple connectomes. Future work will investigate automated approaches to identify and highlight meaningful patterns within connectome datasets.

ConnectoVis is available via our open source GitHub code repository at `https://github.com/CreativeCodingLab/ConnectoVis`, along with source code, detailed instructions on how to load in custom datasets, and additional documentation.

Chapter 4

Dynamic Connectome Classification using Graph Neural Network

4.1 Introduction

Over 300 million people worldwide suffer from depression, and over 700,000 people die due to suicide every year, according to the World Health Organization (WHO). Several large-scale studies have been conducted to determine how the depressive brain functions differently from a normal brain and whether psychological treatments are effective. Understanding the functional activities of the human brain is crucial for understanding cognition and behavior patterns. A common way to study functional brain activity is to use non-invasive brain imaging techniques such as functional magnetic resonance imaging (fMRI).

fMRI measures brain blood oxygenation levels by detecting changes associated with

blood flow. The result from the fMRI scan is used to derive the functional connectivity (FC) between brain regions. There are two major types of FC: static Functional Connectivity (sFC) and dynamic Functional Connectivity (dFC). Initially, researchers assumed no change in functional connections during resting state [33]. A majority of the studies used statistical characteristics of time series reading to detect anomalies in the brain pattern. By folding the temporal dimension of dFC, the manually selected features overlooked time-varying patterns during the analysis. Recent studies have found that analysing temporal functional activities reveals hidden insights of various brain disorders such as Alzheimer's Disease [30], Depression [36], Schizophrenia [69].

The inclusion of temporal information adds an additional layer of complexity to this analysis since it is difficult to manually keep track of the changes in the connectivity between nodes per time step. Visualization tools can help researchers see dynamic connections between brain regions, however, as the number of time step increases it is difficult to track the long-range trends making the process of identifying unhealthy brains tedious. Moreover, the complexity increase exponentially when observing connectivities between multiple brain regions over time.

In recent years, machine learning has proved useful in analyzing complex data in a wide range of fields, including neuroscience. In computational neuroscience, machine learning is mainly used for classifying a healthy brain from an unhealthy one by looking at the representative features of the experiment groups. The majority of machine learning models for depression analysis, however, relies on static functional connectivity (sFC) obtained from correlation analysis of fMRI time series activities and ignores tem-

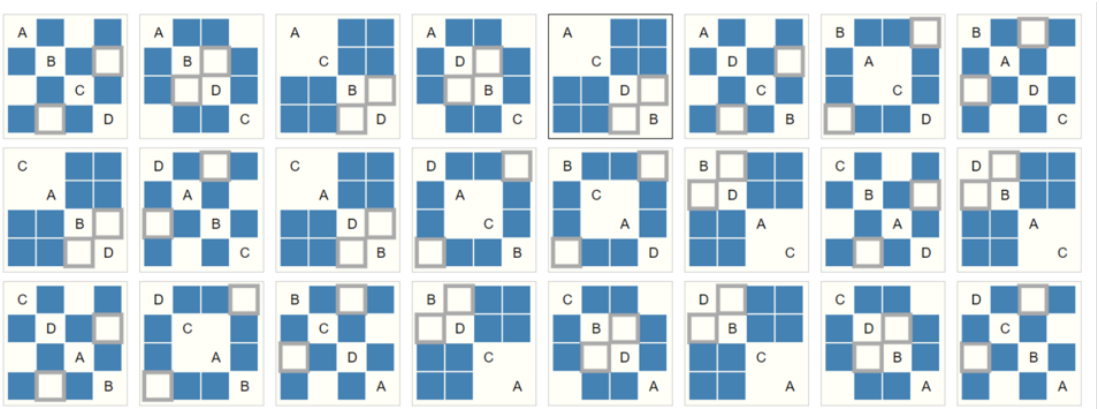

Figure 4.1: Example of different adjacency matrix representing the same graph [60]

poral characteristics. The commonly used model for classifying mental disorder group and health controls is support vector machine (SVM). SVM is a supervised learning techniques that works by constructing a decision boundary separating the data into two groups by reducing a cost function. SVM is not directly suitable with timeseries data and require several data transformation steps resulting in loss of features. Yan et al. used SVM to classify dynamic functional connectomes and highlighted 28 functional connections which are distributed in different time window. This model fails to provide insights of dynamic fluctuation of connectivity from the result [75]. Neural network models are now experimented in static connectivity analysis [37] but rarely used for dynamic brain networks. To the best of our knowledge, only one work has been done based on dynamic functional connectivity (dFC) for classifying gender, where they combine a convolutional neural network (CNN) with a long short term memory (LSTM) in order to capture the temporal features [18]. CNNs are the state of art neural network for analyzing patterns in images. However, dynamic functional connectivity consists of series

of nodes and edges forming a chain of graphs. This connection graph is represented as an adjacency matrix with row and column representing vertex and value represent the edge weight. There are two main disadvantages when using adjacency matrix as the input to a CNN model. CNNs are inherently not permutation invariant which means that each adjacency matrix input looks different to the model. The same functional connectivity data can be represented using a number of adjacency matrix as shown in Figure 4.1 but the model fails recognize it as the same graph representation. Training such a network on adjacency matrix data makes it hard to converge and leads to poor generalizability of the model on test data [60].

Graph Neural Networks (GNNs) are permutation invariant model that learns feature vectors for nodes, edges, or the entire graph. GNNs are used in graph analysis for social network [19], transportation data [14] and drug discovery [15]. GNN take a graph as the input (adjacency matrix) consist of several node and edges that connects the nodes and output a new graph. The nodes and edges can carry features which is then transformed into a learned embedding for the output graph. The output graph can be then used for node classification, edge prediction or classification of an entire graph. The core idea of GNN is to use a series multi-layer perceptron (MLP) or fully connected network on each node (or edges) to extract the features. The same MLP is applied to all the nodes and the features are combined in a message passing step. In message passing the connected nodes share features which are aggregated using a permutation invariant operation such as sum or average. If the GNN have multiple layers i.e. multiple MLPs chained together then with message passing each node receives features from far away

nodes through mutually connected node. For this reason, GNN with message passing are also called Graph Convolution Networks (GCNs) [56]. GNNs are a good fit to analyzing brain functional connectivities since FC can be described as graphs that are composed of nodes (vertices) denoting brain regions that are linked by edges representing functional connections [12].

Since we are working with medical data, we need to validate the model by understanding the working of the classifier, in our case, it means we want to understand which nodes are responsible for the decisions made by the classifier. Mask has been used successfully in explaining GNN model. There were different types of masks: edge mask, feature mask, and node mask. In our model, we used edge connectivity in the node feature, so in order to highlight the significant brain regions for classifier, we applied a learnable node mask. However, message passing aggregated the node features with their neighboring nodes at every layer. So the mask for each node won't represent for individual node. Hu et al. showed that message passing in GNN is not necessary for classification. Instead, they encode the graph structure information into the node features[32]. Motivated by their work, we removed the message passing part in GNN and designed a new recurrent graph network for temporal connectome.

Using the designed GNN model for dFC with graph recurrent connections, we will show its capability to classify a remitted depression group from healthy control group. In summary, We introduce a new data analysis pipeline that is specifically designed for dFC data. Our contributions are:

- A novel Temporal GNN model classifying remitted depression vs healthy dynamic

connectomes.

- To improve the explainability of our model, a mask is generated per connectome to identify the regions responsible for the classification.
- Support for visualizing the results from the model in *Tempocave* for analysis or verification by a domain expert.

4.2 Spatio-Temporal Network Analysis using GNNs

4.2.1 Dataset

The dataset is from an ongoing clinical study that measures the effectiveness of rumination cognitive behavioral therapy (R-CBT) for adolescent patients with at least one previous episode of major depression disorder (MDD) [13]. In this study, 27 patients were recruited for comparing 8 weeks of R-CBT data against a control group of 15 healthy participants. The patients were in remission at the start of the study, and the main goal of the study was to measure the effectiveness of R-CBT at preventing a relapse of depression. 27 patients that have previously diagnosed as MDD had all relapsed of depression in the beginning of the experiment. We used the baseline for our model by classifying 15 health control with 26 MDD remission (We have deleted one connectome due to corrupted data). Each connectome was partitioned into 105 brain regions. Each brain region is treated as a node. The connectivity between brain regions are treated as edges, and the connections are the edge weight. 16 time steps were processed by sliding window Pearson correlation, and each time step is a 105*105 connectivity matrix. We

also included the spatial location into the node features. The dataset was then separated into node features and edge features as input of GNN model. Figure 4.2 shows an example of node features of one time step in one of the temporal connectomes. Each row represents the features of one brain regions during one time step. The columns highlighted in green are the node positions, and the symmetric matrix on the right side is the functional connectivity of each node in one time step.

4.2.2 Model

Our model, as shown in Figure 4.3, is composed of a 2 layer GNN, a graph recurrent connection and a fully connected classifier. The input to the GNN is the dynamic connectome graph and the model outputs a transformed graph with learned temporal features for each node. The temporal features of each node are concatenated and send to a fully connected network for classification.

The input graph consist of 105 nodes and each node carries a feature vector of size 108 containing the 3D spatial location of the node and the edge weights to every other nodes at each time step. For a time step of 16, we will have the input graph of size 105x108x16.

Our graph neural network (GNN) consist of two layers that are shared among all the input nodes. Each GNN layer is a 2-layer MLP with ReLU as the activation function. After each layer a message passing step will aggregate the feature from the immediate neighbor node. Although our experiments with message passing have been successful, we dropped the message passing mechanism in our GNN in favor of model explainability as

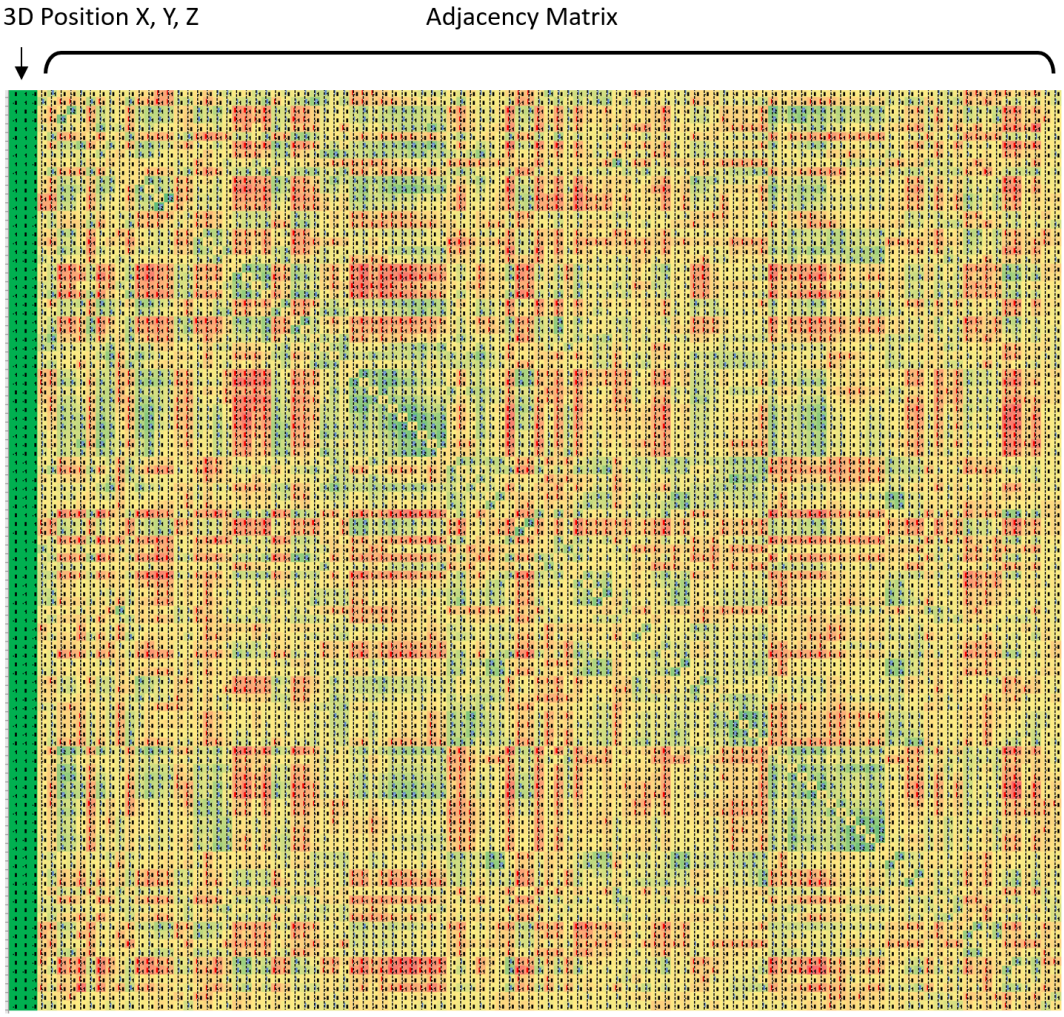

Figure 4.2: Example of node attribute: one time step of one of the connectome node attribute input. The first three columns (in green) are the node positions, and the symmetric matrix on the right side is the functional connectivity of each node in one time step.

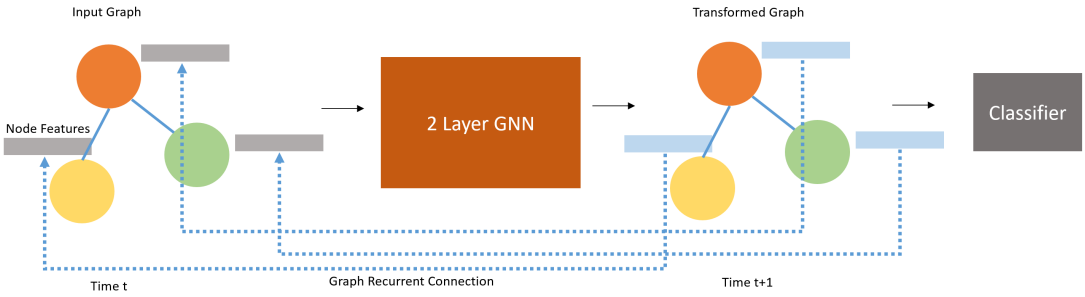

Figure 4.3: Overview of our model consisting of a GNN, graph recurrent connection and a classifier

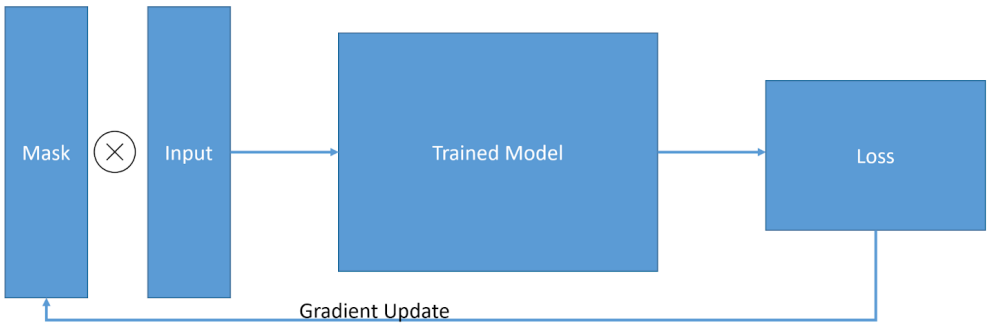

Figure 4.4: Mask generation pipeline

described in Section 4.4.1. Recent studies have indicated that GNN can achieve similar accuracy without a message passing technique [32, 71]. The modified GNN looks similar to a standard MLP except that the same layers are applied across all the nodes. There are 3 reasons why we prefer a GNN over a bigger single MLP:

- With shareable weights GNN scans for same features over all nodes (similar to a kernel in CNN) which allows preserving graph symmetry and this is not guaranteed with a single MLP where the input is reduced into a single vector.

- With MLP the node features across the timesteps are flattened and given the input to the network requiring a very large number of weights to be trained which is expensive to compute and difficult to converge while our GNN model learns temporal features for each node iteratively with less number of parameters.

- The standard MLP expects a fixed input size which means that if the number of time-step increases a new MLP need to be trained from scratch. With our graph recurrent connections, the GNN model can process connectomes with a variable timestep.

For getting temporal features, we considered using recurrent neural networks (RNN), long short term memory (LSTM). RNNs suffer from a vanishing gradient problem where the gradients are multiplied by values close to 0 after learning long sequences, which make it not scalable to long time steps. LSTM models avoid vanishing gradients, but their interpretation capability remains unclear, which makes the model difficult to explain [18]. We propose a graph level recurrent network where the node feature from

the previous timesteps are concatenated with the input node feature of the current timestep. The temporal features improve iteratively after each timestep. An advantage of using graph recurrent networks is that they do not store temporal states like RNNs or LSTMs, which affect explainability. Similar recurrent connections are used in video processing networks that motivated us to adapt it to a graph network [59, 20].

Finally, the learned temporal features of all the nodes are concatenated into a single feature vector and send to a fully connected network for classification. The classification network consist of 3 layers with ReLU as the activation function. The output is a single value determining whether the input is an healthy connectome or not. The network is trained using a binary cross entropy loss with a learning rate of 0.0001 for 1000 epochs.

Once the training is finished, a mask generation techniques is used to find the nodes responsible for the classification. The mask generation algorithm (shown in Figure 4.4) works as follows:

1. Set the GNN to inference mode, i.e. weights are not trainable.
2. Initialize a mask per node with random weights clipped to 0 (off state) or +-1 (on state) based on a threshold.
3. Multiply the mask with the node features.
4. Run the model with the masked graph.
5. Calculate the L1 loss between the prediction and ground-truth.
6. Update the mask by back propagating through the network.

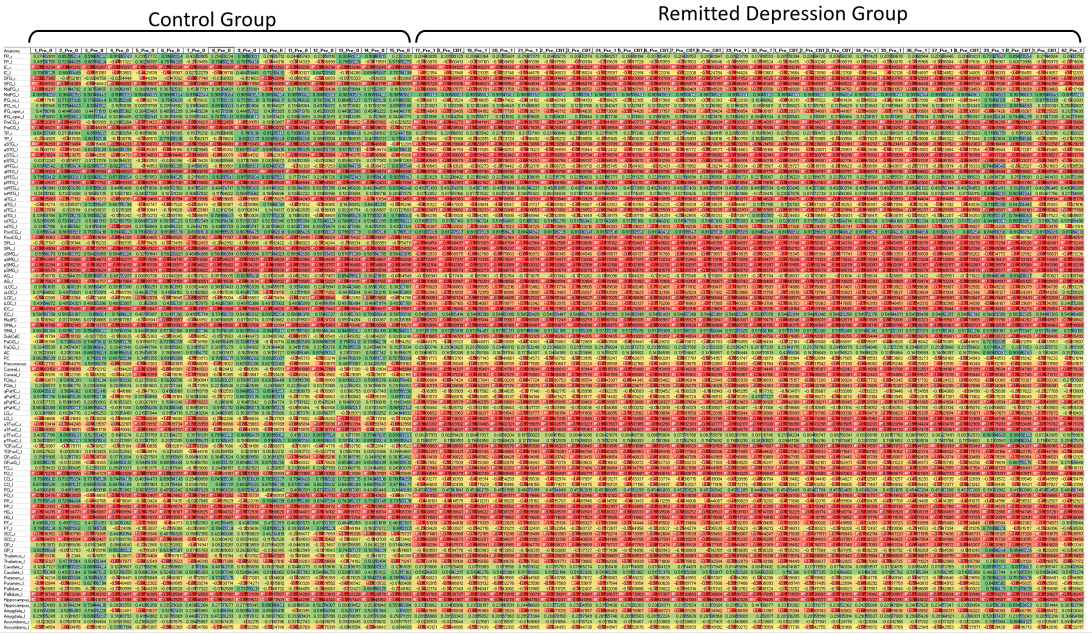

Figure 4.5: Original mask weights for control and remitted depression group

7. Repeat the process until the loss is minimized.

4.3 Results

We split the data (26 remitted depression patients and 15 healthy controls) into training (22 remitted depression patients and 11 control group) and test group (4 remitted depression patients and 4 healthy controls). The accuracy of our model is 98% after around 100 epochs of training. Precision recall curve is shown in Figure 4.7 with Area Under Curve (AUC) value 0.96. Using the trained classifier, we generate the mask and apply it on the node features to get the weight for each brain region. The weight for each brain region represents the contribution of that region for the classification. We exper-

imented with a range of mask activation functions to get distinctive patterns. Initially, we used a sigmoid function to get mask range of [0,1] but in our experiments we found this range hard to distinguish the contribution of brain regions. Using tanh activation function we increase the range of the mask produced to [-1, 1], showing clear difference between depressive connectome and healthy control connectome. As shown in Figure 4.5, participants number 1-15 are from control group and they are located on the left side of the chart, and participants on the right side are remitted from depression. The mask value are color coded and the mask value of healthy control and depressive group has a clear division shown in the figure 4.5. By subtracting the mask value between the two groups, we get an average mask difference for each node. The mask difference can be considered as the discriminative power for the classification of the two group. Using our mask mechanism, we narrow down the 105 brain regions to 42 that is contributing to the classification. The mask difference is in the range of [0, 1.21], with aSMG_r demonstrate the highest value. Following aSMG_r, other brain regions that have high mask difference are: iLOC_l, CO_l, IFG_oper_r, CO_r. Our findings are supported by various depression studies done by different neuroscience research groups. For instance, supramarginal gyrus (SMG) showed increased amplitude of low-frequency fluctuation (ALFF) in depression groups [46]. Right central opercular cortex was found increased activities in depression patient [40].

We convert the mask with continuous weights to a discrete value using a threshold. Through our experiments we found applying +-0.7 threshold on the mask to work the best without influencing the accuracy. Figure 4.6 shows the mask after applying thresh-

old. Note that participants number 1 -15 are control group, and they are located on the left side of the chart, and participants on the right side are remitted from depression. If the mask value is 0 for a brain region, then it is not used in classification. If the mask value is 1 or -1, then the brain regions are important for the model for classification. As shown in the Figure 4.6, each connectome produces a different mask vector (105x1) to be classified correctly showing that our model can extract features from different brain region and not overfitting to one region for the classification. Interestingly, for all depressive connectomes the mask vectors suggest that the model is focusing on the same brain regions. We firstly focus on group level difference by labeling the different brain region mask between health control and remitted depression patients. Based on our analysis of network outputs and mask weights for 105 brain regions, 33 brain regions show strong differences between the two groups.

4.3.1 Visualizing the Results in *ConnectoVis*

We will demonstrate the connectivity and modularity dynamics using *ConnectoVis* for the top brain regions identified using our model and mask mechanism. As shown in Figure 4.8, aSMG_r more positive connections comparing control and depressive group on average. We will focus on positive connections using *ConnectoVis*. We randomly select subject 5 and 9 from control group, and 18, 26 from remitted depression group, with brain region aSMG_r selected. The figure 4.10 shows the positive connections from aSMG_r to other regions at t = 1, 4, 8, 15. Overall, subject 5 and 9 shows lower positive connections from aSMG_r to other regions and less fluctuations as well. However, subject

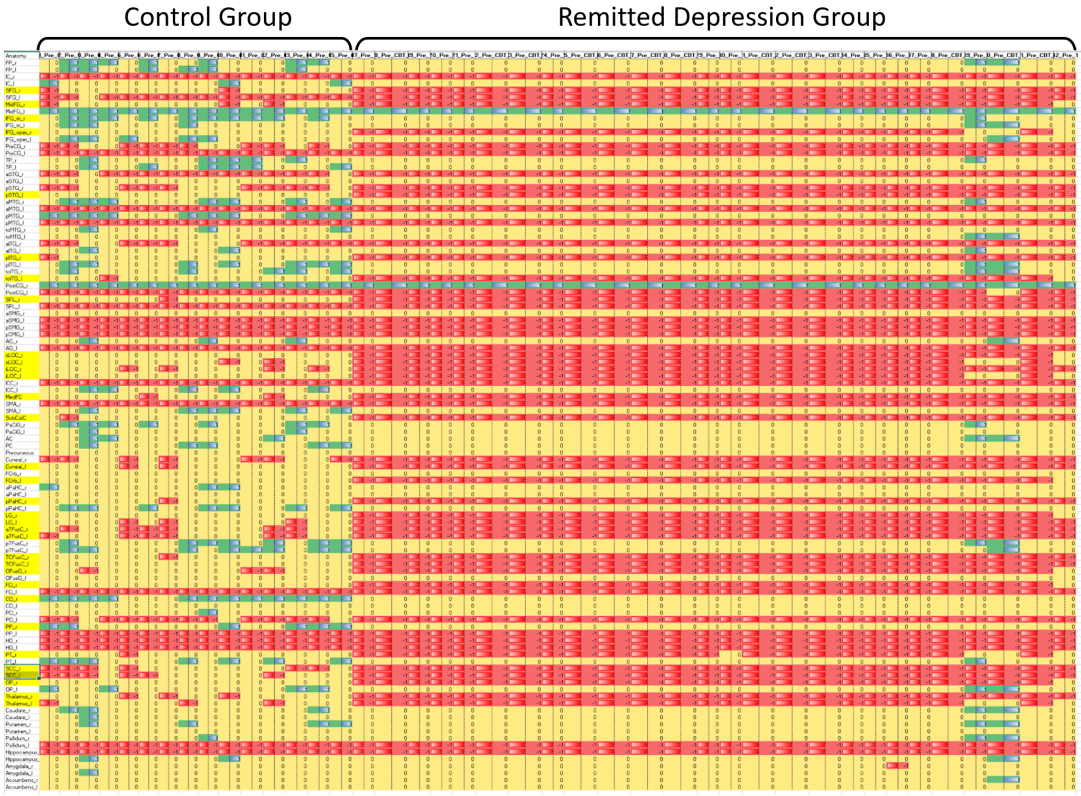

Figure 4.6: Discrete mask weights in the range [-1,1] for control and remitted depression group

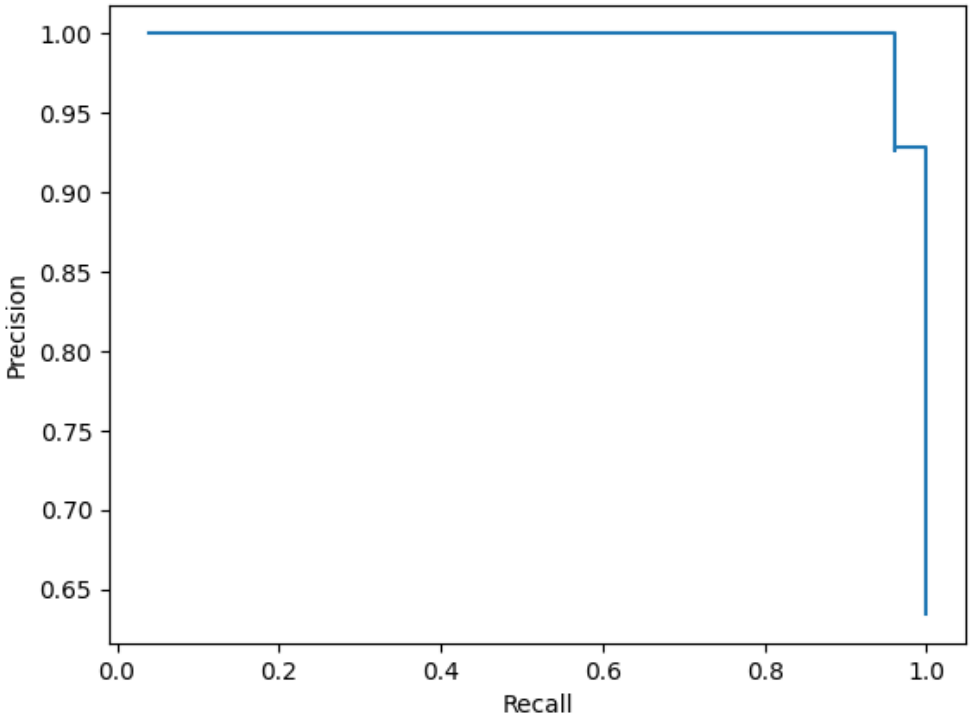

Figure 4.7: Healthy control and remitted depression group classification Precision Recall Curve, AUC is 0.96.

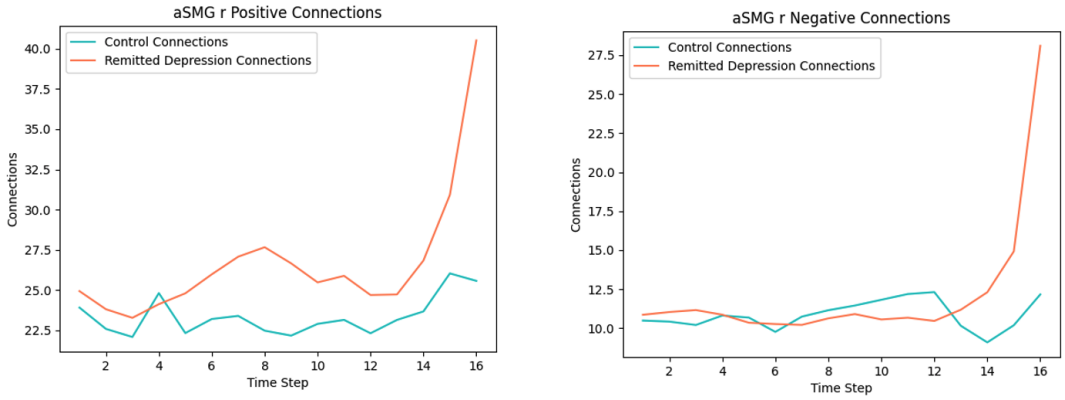

Figure 4.8: aSMG r connectivity strength over time in control vs remitted depression group

18 adn 26 shows more positive connections overall and more fluctuations over time. When looking at the modularity changes over time, we see more flexibility in subject 5 and 9 compare to subject from remitted depression group in the region aSMG_r, as shown in Figure 4.9.

4.4 Discussion

4.4.1 GNNs Explainability

Message passing is a powerful mechanism to aggregate features from the neighboring nodes using permutation invariant operators. In our initial model, we used message passing to generate a graph level representation for each time step without using recurrent connections. The graph representation across all time steps are concatenated and send to the fully connected network for the classification, as shown in Figure 4.11.

Figure 4.9: *ConnectoVis*: aSMG r modularity change over 16 time steps for subject 10 (control group), 18, 30, 31 (remitted depression)

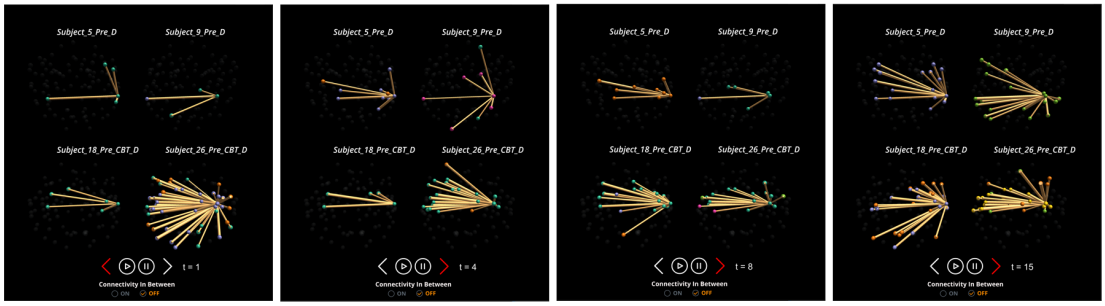

Figure 4.10: *ConnectoVis* shows aSMG r connectivities over 16 time steps for subject 10 (control group), 18, 30, 31 (remitted depression)

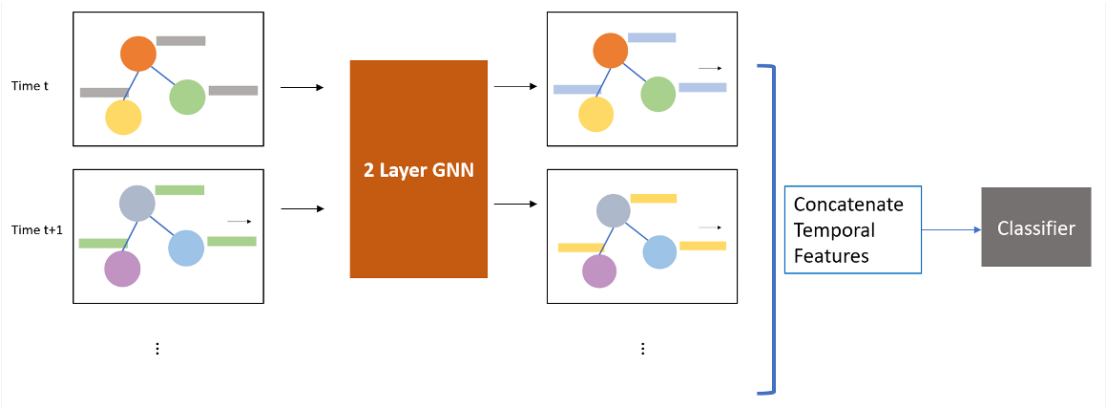

Figure 4.11: GNN model with message passing

The model achieved high accuracy similar to our current technique but its features has poor explainability. In our experiments with the mask generation pipeline, we found that the mask weights are only active for few selected nodes that are fixed across all the connectomes. On further investigation with the features, we found that the reason is message passing blended the information from multiple nodes and aggregated to a couple of master nodes. Those master nodes are enough to classify, so we won't get distinct features for each node.

4.4.2 HCP Gender Classification using Our Model

To validate our model, we used our network on a larger publicly available dataset from Human Connectome Project (HCP) for gender classification [65]. This dataset consists of participants between the ages of 22 and 35 without a history of mental illness or neurological dysfunction. The dataset provides pre processed static connectivity matrix for individual subjects and individual subject's resting state fMRI timeseries data. For each subject's fMRI timeseries data, participant connectome is partitioned into varies number of brain regions with 4800 time points for each region. We chose 100 number of nodes for our experiment. For extracting the temporal connectivity matrix we used the time series signal of 812 participants and applied a sliding window Pearson correlation. Out of 812 subjects, there are 410 female and 402 male.

Our model achieves an accuracy of 93% for gender classification on the temporal connectivity matrix similar to the CNN+LSTM model [18] while SVM classifies with an accuracy of 75.1%. We also performed training on the preprocessed static connectome data by removing the graph recurrent connection. Our model achieves an accuracy of 95% for gender classification task. In comparison to dynamic connectomes, static connectomes perform better due to limitation in our data processing which affects the quality of the temporal connectivity matrix since we used reduced temporal resolution of 17 time steps for a faster training time.

4.4.3 Comparison with BrainNetCNN for Classifying Temporal Connectomes

BrainnetCNN provides alternative custom convolutional layers designed to process brain network data [37]. The edge-to-edge layer compute the weighted activation over the neighboring edge for a given edge. The edge-to-node layer similarly computes a weighted activation over neighboring edges for a given node. Classification is completed by connecting all of these activations to a fully connected network. While BrainnetCNN is developed for static connectome classification, for validating it's performance with temporal data, we extend the custom layers to process 3D data by adding an additional dimension which contains the time-varying data. The network failed to converge on our rumination dataset as shown in. Our finding suggests that the custom layers are not suited for processing temporal information.

4.5 Conclusion

In this work, we have proposed a novel temporal connectome data analysis pipeline using Graph Neural Network. Our model supports explainability providing the list of nodes responsible for the classification. We use a mask generation technique to assign weights on the important nodes. Using our model, we show the difference between remitted depression patients and healthy controls that align with the various neuroscience studies. The results can be visualized on our *ConnectVis* platform by a neuroscientist to verify the network outputs. Our tool has many applications ranging from auto-labeling

to discovering new regions related to brain disorders.

4.5.1 Limitations and Risks

Our model can be used in a wide range of applications in neuroscience and non medical domains, such as social media studies and transportation networks. However, there are some limitations and risks associated with our model due to bias and black box nature of deep learning techniques. In neuroscience application, this can lead misdiagnose of diseases. We provide tools such as the model explainable mask and visualization applications for the neuroscientist to verify the predictions. There will be some bias in the model depending on gender, race, age of the training data. Collecting a large amount of data from wider population help reduce the bias in the system. Training on large dataset will require higher energy usage increasing the cost of training. An option to reduce the cost is to do fine tuning the model instead of training from scratch when new data is collected.

Chapter 5

Use Cases

In this section, we will demonstrate three detailed use cases in the neuroscience domain for analyzing and visualizing dynamic connectivities between brain regions. In all three use cases that are discussed here in this section, we follow the steps:

- We train our temporal GNN model on a dynamic connectome dataset for extracting temporal features. The features are used to classify disease group from control group.
- After the model training is complete, for each connectome we run the differentiable mask generator to find the regions of interest.
- Using our visualization platform, we verify or explore the findings from the model for disease vs control group, or for pre vs post treatment using the overlap comparison feature.

5.1 Use Case 1: Cross Network Connectivity Comparison Between Healthy Control and Remitted Depression Patients

We train our model on the dynamic connectomes from 26 remitted depression patients and 15 healthy controls and applied our mask generator. Each connectome consists of 16 time steps and 105 brain regions. Using this dataset, our temporal GNN model successfully trained to classify healthy control and depression group with an accuracy of 98%. After setting GNN to inference mode, a mask in the range of [-1, 1] is then generated for each node. The mask is now based on individual level, i.e. each brain region of every connectome has a unique decimal mask in the range [-1, 1] assigned to it. In order to get the relevant brain regions for classification, we get a group average mask for each brain region and rank the average difference of the two groups, and the results is shown in table 5.1. The mask average difference can be considered as the discriminative level for the classification of two groups. The top brain region aSMG_r is right anterior supramarginal gyrus, and the mask difference between two group is 1.21. This difference is the subtraction of the group average mask for control group (0.55) and the group average mask for depression group (-0.66). This result is consistent with study from Zhu et al. where they stated: "supramarginal gyrus exhibited high discriminative power in classification" [80].

In Zhu et al.'s study, cross network connections (connections across different brain networks) among the default mode network (DMN), salience network (SN), central exec-

utive network (CEN) and visual cortical network (VN) showed higher connection weight for depression patients. From our results in Table 5.1, brain regions from above networks have been narrowed down to MedFC, PC, aPaHC_l, pPaHC_r, and pPaHC_l from DMN, IC_l, Amygdale_r, pSTG_l, and aSTG_l from SN, LG_l, LG_r, OFusG_l, OFusG_r, TOFusG_l, and TOFusG_r from VN. The overall absolute sum of the connections within those regions have higher value for depression group than healthy control. Over 16 time steps, the average brain connections among healthy control and depression group are shown in Figure 5.1. From the figure, both positive and negative connections increased dramatically towards the end of the time step for depression group. And overall, depression group has higher negative connections than healthy control on majority of the time points. In order to find out the details of cross network connections over time, neuroscientists use *ConnectoVis* to observe the modularity and connection dynamics. For instance, when observing negative connection with node modularity dynamics, we set the threshold of edge connections to negative with the brain region above selected, and show connections in between the selected regions, as shown in Figure 5.2. From the figure, subject 6 and 8 are healthy control and subject 38 and 40 are depression patients, navigating through different time steps, depression patients shows increased negative connections between regions selected. At the same time, with the node color representing the module, we see that negative connections increase among both same module and different modules in depression connectomes. Also, left panel in Figure 5.2 is the modular dynamics of MedFC, Amygdale_l, and LG_r. Brain regions within the same network mostly belong to the same module, for instance, the MedFC, PC from

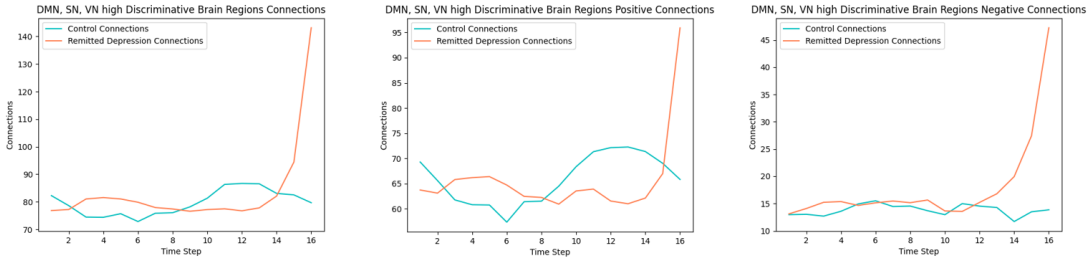

Figure 5.1: Use Case 1: Connections cross network of DMN, SN, VN for healthy control and remitted depression group. The left image is the absolute average of both positive and negative connections for the two groups over time, middle image is positive connections only, and right image is the absolute negative connections.

DMN has same module on majority of time steps. So we choose one region from each network: i.e. MedFC from DMN, Amygdale_l from SN, and LG_r from VN, to compare modular dynamics. The red rectangle highlights the time ranges that those brain region belong to same module. From the figure, depression patients share longer time of same modules among different networks.

Brain Regions Abbr.	Region Full Name	Mask Average Difference Between Two Groups
aSMG_r	Supramarginal gyrus, anterior division right	1.21
iLOC_l	Lateral occipital cortex, inferior division left	1.15
CO_l	Central opercular cortex left	1.14
IFG_oper_r	Inferior frontal gyrus, pars opercularis right	1.13

Brain Regions Abbr.	Region Full Name	Mask Average Difference Between Two Groups
CO_r	Central opercular cortex right	1.12
sLOC_r	Lateral occipital cortex, superior division right	1.09
toITG_l	Inferior temporal gyrus, temporooccipital part left	1.07
LG_r	Lingual gyrus right	1.03
FO_r	Frontal operculum cortex right	1.01
PT_r	Planum temporale right	0.99
FOrb_l	Frontal orbital cortex left	0.98
FOrb_r	Frontal orbital cortex right	0.96
Amygdala_r	Amygdala right	0.95
pPaHC_r	Parahippocampal gyrus, posterior division right	0.94
PC	Cingulate gyrus, posterior division	0.90
OFusG_r	Occipital fusiform gyrus right	0.88
pSTG_l	Superior temporal gyrus, posterior division left	0.87
sLOC_l	Lateral occipital cortex, superior division left	0.87
MidFG_r	Middle frontal gyrus right	0.87
OP_r	Occipital pole right	0.85
TOFusC_l	Temporal occipital fusiform cortex left	0.84
OFusG_l	Occipital fusiform gyrus left	0.84
IFG_tri_r	Inferior frontal gyrus, pars triangularis right	0.81

Brain Regions Abbr.	Region Full Name	Mask Average Difference Between Two Groups
PaCiG_r	Paracingulate gyrus right	0.79
pITG_r	Inferior temporal gyrus, posterior division right	0.76
MedFC	Frontal medial cortex	0.74
aSTG_l	Superior temporal gyrus, anterior division right	0.70
PP_r	Planum polare right	0.65
SubCalC	Subcallosal cortex	0.64
SPL_r	Superior parietal lobule right	0.64
aMTG_r	Middle temporal gyrus, anterior division right	0.64
aPaHC_l	Parahippocampal gyrus, anterior division left	0.64
SFG_r	Superior frontal gyrus right	0.63
pPaHC_l	Parahippocampal gyrus, posterior division left	0.61
IC_l	Insular cortex left	0.60
PT_l	Planum temporale left	0.59
FP_l	Frontal pole left	0.56
TOFusC_r	Temporal occipital fusiform cortex right	0.55
Thalamus_r	Thalamus right	0.54
pITG_l	Inferior temporal gyrus, posterior division left	0.52
SCC_r	Supracalcarine cortex right	0.51
LG_l	Lingual gyrus left	0.50

Brain Regions Abbr.	Region Full Name	Mask Average Difference Between Two Groups

Table 5.1: Use Case 1: List of brain regions with mask difference between remitted depression and healthy control associated with each region. (Only > 0.5 difference are shown in this table).

5.2 Use Case 2: R-CBT Treatment Comparison

In this use case, we will demonstrate the effectiveness of our tool for analyzing R-CBT treatment. The dataset consists of 14 connectomes of pre R-CBT treatment remitted depression adolescents and 14 connectomes post R-CBT treatment the same adolescents after 8 weeks of treatment. Each connectome consists of 105 brain regions and 16 time steps. By applying our temporal GNN classification model (accuracy 88%, precision recall curve AUC is 0.84, shown in Figure 5.3) and mask generator, we get a list of brain region with mask difference between the two groups, shown in table 5.2. From the result, brain region pMTG_l have the top mask difference (1.10) and it demonstrates highest discriminative power in distinguishing the two groups. This indicate that the brain region shows different dynamic activities for the two groups. This result is aligned with study from Burkhouse et al., where they studied neural correlates of rumination in adolescents with remitted major depressive disorder and healthy controls by comparing

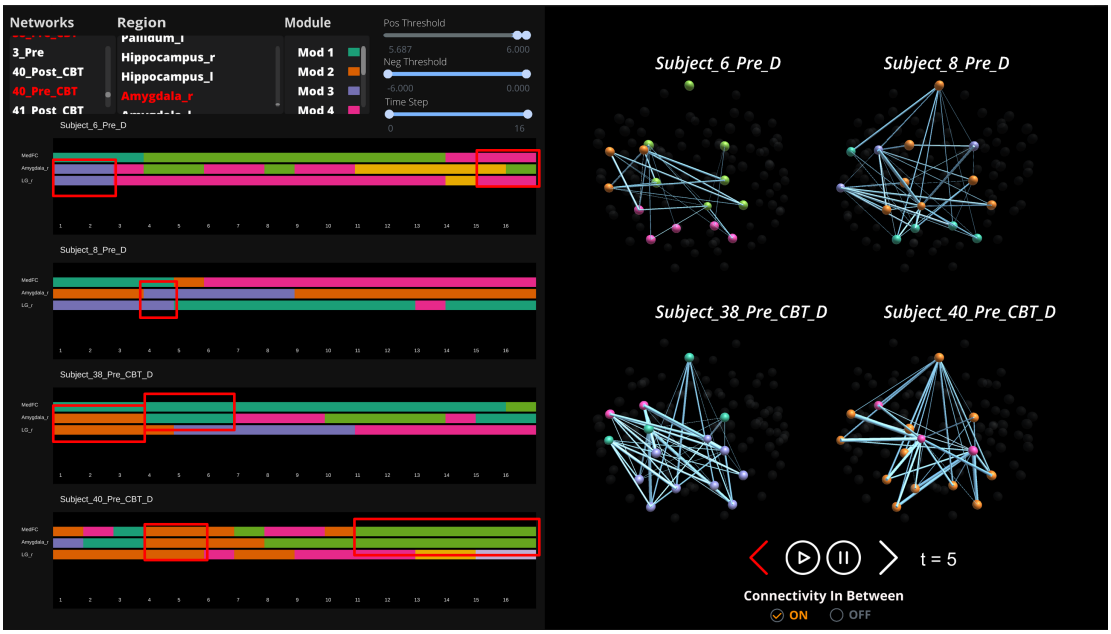

Figure 5.2: Use Case 1: *ConnectoVis*: Connections among brain regions: MedFC, PC, aPaHC_l, pPaHC_r, and pPaHC_l from DMN, IC_l, Amygdale_r, pSTG_l, and aSTG_l from SN, LG_l, LG_r, OFusG_l, OFusG_r, TOFusG_l, and TOFusG_r from VN for subject 6, 8 (healthy control) and 38, 40 (remitted depression group). The left part is the modular dynamics from MedFC, Amygdale_l, and LG_r, and the right part is the connections between the brain regions above with only negative threshold selected at time step 5.

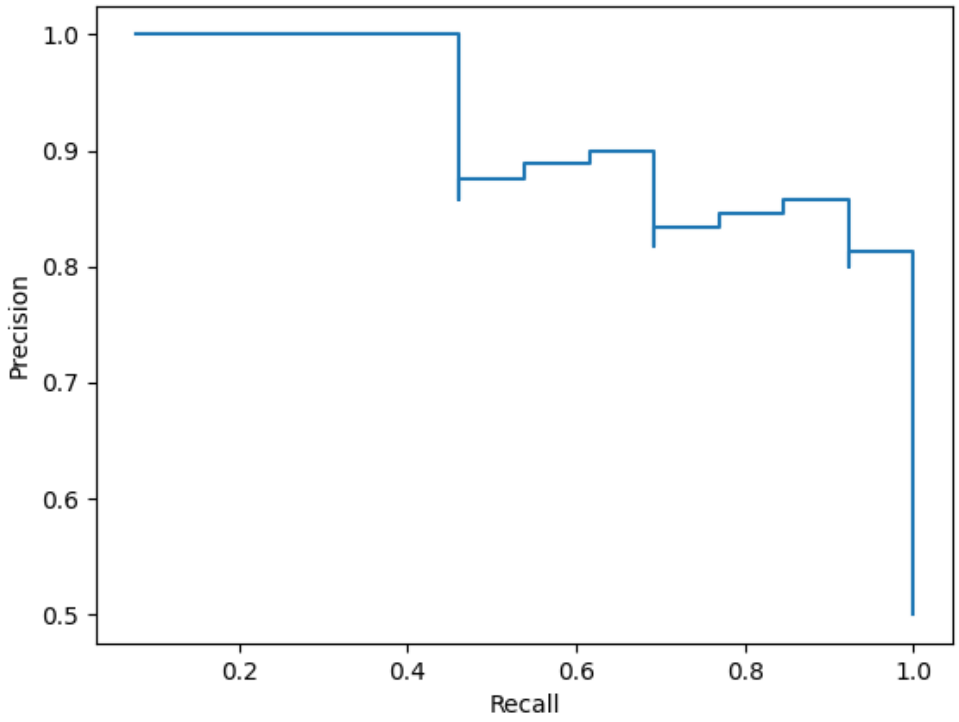

Figure 5.3: Use Case 2: Pre vs Post R-CBT treatment classification precision recall curve, AUC is 0.84.

26 adolescents and 15 healthy controls [13]. In the study, they found that MTG showed increased activation during rumination and the activation is positively correlated with the self reported rumination score.

Similar to use case 1, by selecting different brain regions from table 5.2 in *ConnectoVis*, neuroscientists will be able to check the different activities comparing patients from pre vs post R-CBT treatment. From Figure 5.4, on the left chart, you can see that on average, the negative connections are less for post treatment patients, whereas on

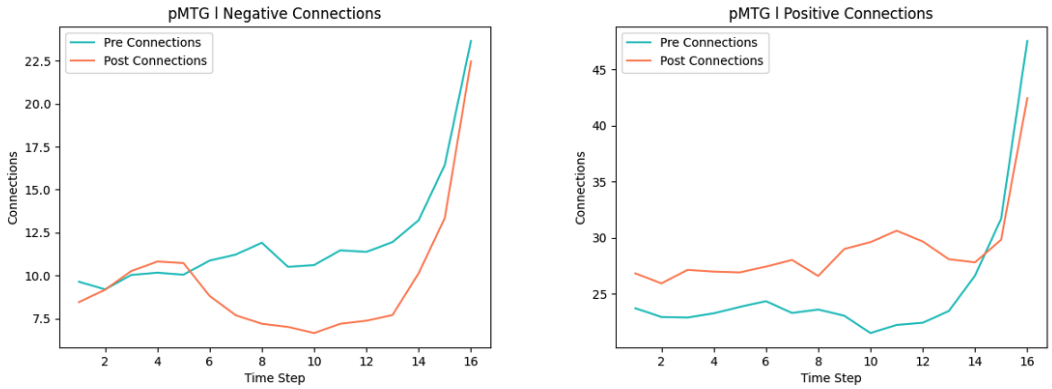

Figure 5.4: Use Case 2: pMTG_l group average connectivity difference between pre vs post R-CBT treatment

the right chart, it shows positive connections increased for post treatment patients. By using *Connectovis*, neuroscientists can check the detailed connections from middle temporal gyrus, shown in Figure 5.5. In this example, we have subject 33 pre treatment and post treatment selected, and the top three images shows positive connections at t = 12, 13, 14, and the bottom three images shows negative connections at t = 7, 8, 9. By choosing different connectivity threshold, neuroscientists can identify the exact decreased negative connections or increased positive connections between pre vs post treatment connectomes.

From the result of the mask, each individual patients demonstrate different set of brain regions that are discriminative between their pre and post treatment. Table 5.3 is an example of different results for subject 18 and 33. Studies found that functional connectivities can be seen as fingerprint for individuals [22]. Even though certain mental

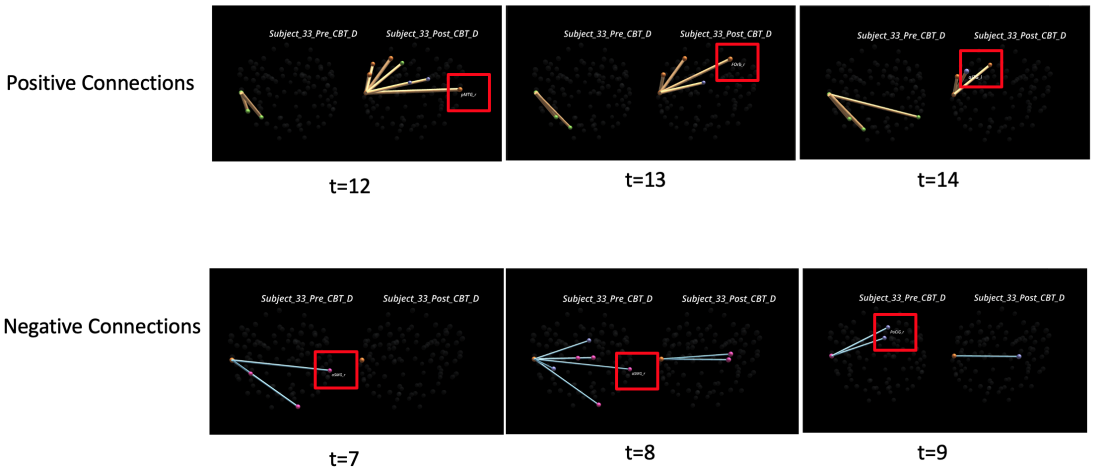

Figure 5.5: Use Case 2: *ConnectoVis*: pMTG_l connectivity for subject 33 pre and post R-CBT treatment connectome

disease patients show common brain activity deficit, individuals can show variations from group activity patterns. From table 5.3, by comparing subject 18 pre treatment vs post treatment, the brain regions pMTG_l, Hoppocampis_r, OFusG_l, and TP_r showed obvious difference from mask, whereas for subject 33, IFG_oper_r, Thalamus_l, iLOC_r show obvious difference on mask for pre vs post treatment connectomes. Figure 5.6 shows the connections from IFG_oper_r, Thalamus_l, iLOC_r for subject 18 and 33, both positive and negative connections from the three regions have obvious difference in subject 33 than 18. Using *ConnectoVis*, we can compare the detailed connections through time. As shown in Figure 5.7, with IFG_oper_r, Thalamus_l, iLOC_r selected and connection strength set to >1, subject 33 post treatment showed higher level of positive connections from the three regions especially from iLOC_r, highlighted in red rectangle.

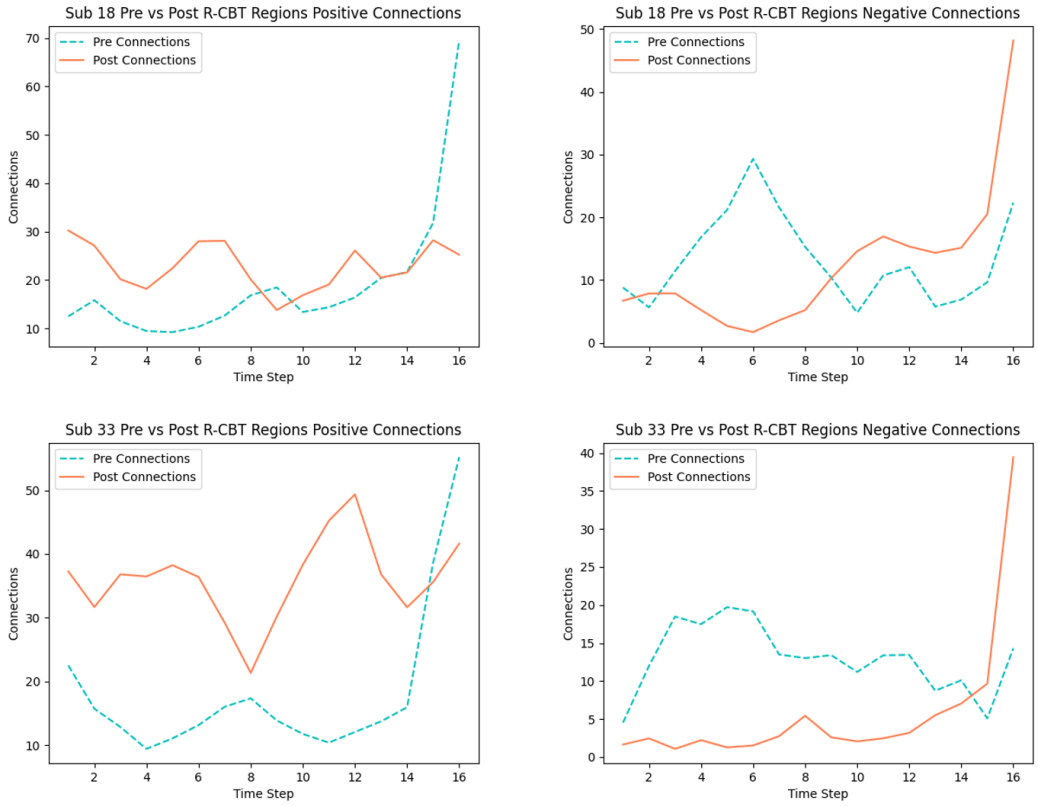

Figure 5.6: Use Case 2: Brain regions IFG_oper_r, Thalamus_l, iLOC_r from patients 18 and 33 of Pre vs Post R-CBT treatment.

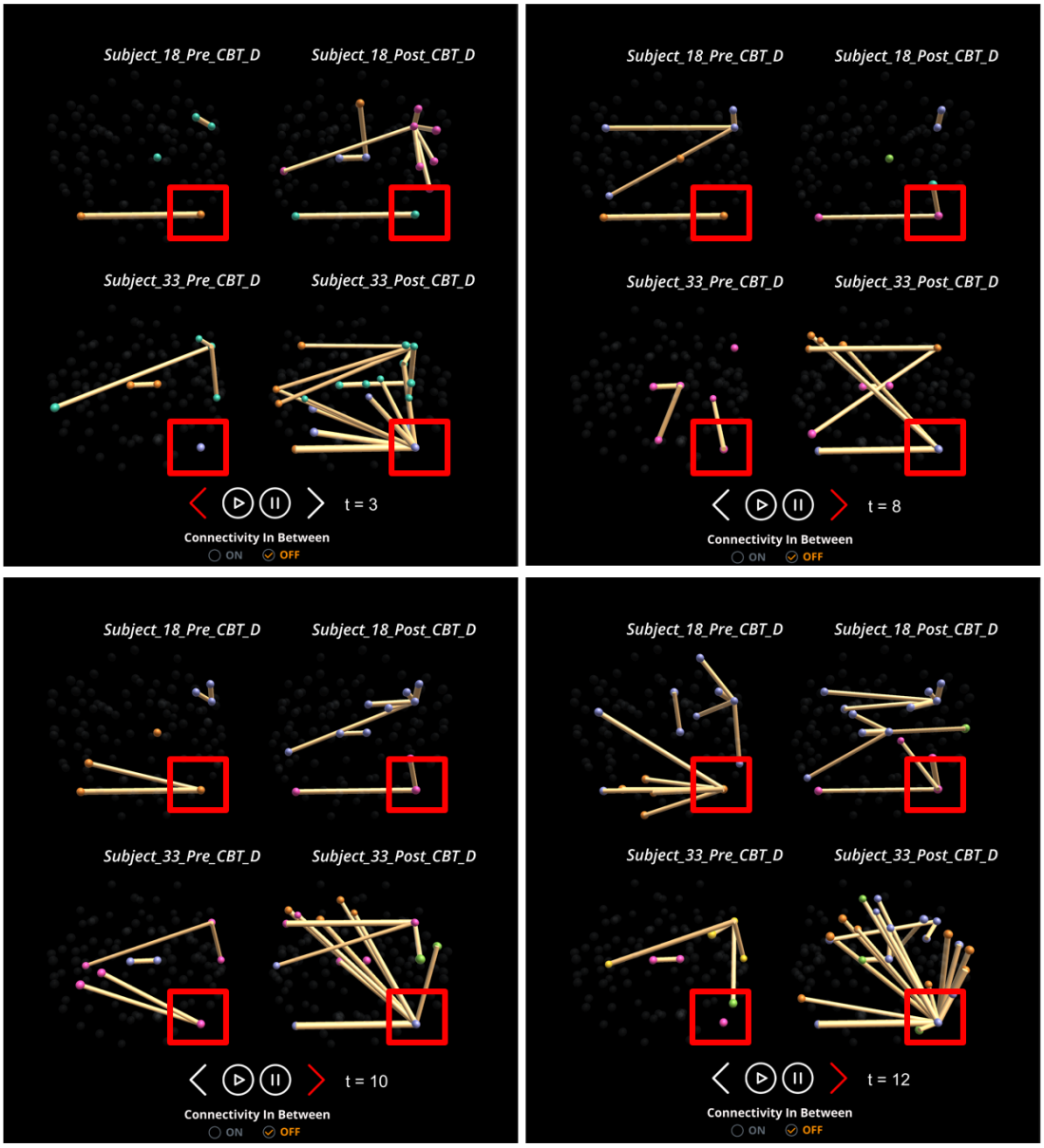

Figure 5.7: Use Case 2: *ConnectoVis*: Brain regions IFG_oper_r, Thalamus_l, iLOC_r from patients 18 and 33 of Pre vs Post R-CBT treatment at time step 3, 8, 10, 12. The red rectangle highlights iLOC_r.

Brain Regions Abbr.	Region Full Name	Mask Average Difference Between Pre Post R-CBT
pMTG_l	Middle temporal gyrus, posterior division right	1.10
aMTG_l	Middle temporal gyrus, anterior division left	0.96
pPaHC_l	Parahippocampal gyrus, posterior division left	0.88
aMTG_r	Middle temporal gyrus, anterior division left	0.85
OP_l	Occipital pole left	0.85
aITG_l	Inferior temporal gyrus, anterior division left	0.84
Cuneal_l	Cuneal cortex left	0.80
Amygdala_l	Amygdala left	0.70
PO_r	Parietal operculum cortex right	0.69
pITG_r	Inferior temporal gyrus, posterior division right	0.68
pITG_l	Inferior temporal gyrus, posterior division left	0.67
HG_r	Heschl's gyrus right	0.65
pMTG_r	Middle temporal gyrus, posterior division right	0.64
CO_l	Central opercular cortex right	0.64
MedFC	Frontal medial cortex	0.63
OFusG_r	Occipital fusiform gyrus right	0.56

aITG_r	Inferior temporal gyrus, anterior division right	0.56
PC	Cingulate gyrus, posterior division	0.55
PT_r	Planum temporale right	0.53
aPaHC_l	Parahippocampal gyrus, anterior division left	0.53
TP_l	Temporal pole left	0.52

Table 5.2: Use Case 2: List of brain regions with mask difference between pre and post R-CBT treatment groups (Only > 0.5 difference are shown in this table).

Subject 18		Subject 33	
Brain Region Abbr.	Mask Average Difference Between Pre Post R-CBT	Brain Region Abbr.	Mask Average Difference Between Pre Post R-CBT
pMTG_l	1.19	IFG_oper_r	1.19
Hippocampus_r	1.15	Thalamus_l	1.19
OFusG_l	1.14	iLOC_r	1.17
TP_r	1.12	pMTG_l	1.17
TP_l	1.12	aMTG_l	1.14
PO_r	1.10	aPaHC_l	1.13
aMTG_l	1.09	FO_r	1.12
pPaHC_l	1.07	aMTG_r	1.11
aITG_l	1.01	pPaHC_l	1.09

AG_r	1.01	OP_l	1.07
pITG_r	1.00	IFG_oper_l	1.04
AG_l	0.98	CO_l	1.03
Thalamus_r	0.95	PT_r	1.01
OP_l	0.94	HG_l	0.99
PreCG_r	0.91	Thalamus_r	0.99
Cuneal_l	0.90	aITG_l	0.97
Amygdala_l	0.89	FP_r	0.94
MidFG_l	0.85	pITG_r	0.94
pTFusC_r	0.85	Cuneal_l	0.88
Accumbens_r	0.83	pTFusC_r	0.87
HG_r	0.82	Pallidum_r	0.86
LG_r	0.81	aSTG_r	0.85
SMA_l	0.80	aTFusC_l	0.85
toMTG_l	0.76	SFG_r	0.84
pMTG_r	0.74	HG_r	0.84
Cuneal_r	0.74	aITG_r	0.82
pSMG_r	0.72	OFusG_r	0.80
sLOC_l	0.68	toMTG_r	0.75
PO_l	0.68	pMTG_r	0.66
Pallidum_r	0.66	MedFC	0.66
HG_l	0.65	SPL_l	0.66
CO_l	0.63	pITG_l	0.66

pITG_l	0.63	IC_r	0.63
PostCG_r	0.62	FP_l	0.58
PP_r	0.61	TP_r	0.57
Putamen_l	0.61	pSMG_r	0.56
toMTG_r	0.59	SFG_l	0.56
CO_r	0.55	FOrb_l	0.53
MedFC	0.54		

Table 5.3: Use Case 2: List of brain regions with mask difference between pre and post R-CBT treatment for subject 18 and 33 (Only > 0.5 difference are shown in this table).

5.3 Use Case 3: Finding Similar Brain Regions from Node Embeddings

The pre-trained GNN model provides feature representation for each node. The feature representation includes the temporal features and can be used to find the brain regions that have similar temporal features with a target brain region within the same connectome. We used the pre trained network from depression vs control classification (Use Case 1) and output the feature representation of each brain region. L1 norm is applied to the feature vectors to get the distance between each node representing the similarity of brain region features. Appendix A table contains the full list of brain regions and their top one region with closest dynamic feature for both control and depression group. For instance, region LG_r have most similar region with LG_l in

control group whereas ICC_r in depression group. Figure 5.8 shows average group dynamics for LG_r and ICC_r. From the figure, LG_r and ICC_l demonstrate more similar dynamic fluctuations for both negative and positive connections in depression patients than in healthy control.

To get the detailed difference, we use *TempoCave* to check compare the negative connections difference of LG_r and ICC_l. When comparing two brain regions, depressive patients show very similar connections, whereas in healthy control, the two regions show slightly different connections. Figure 5.9 is an example of healthy control subject 8 with two brain regions and their negative connections selected. Navigating over different time steps, subject 8 region ICC_l has more various negative connections with iLOC_l, iLoc_r, and OP_r, whereas LG_r doesn't show negative connections with them. This use case demonstrates how neuroscientists can use the brain region similarity result from our machine learning model combining with *TempoCave* to check the similar or dissimilar connectivity dynamics within same connectome between control group and depression patients.

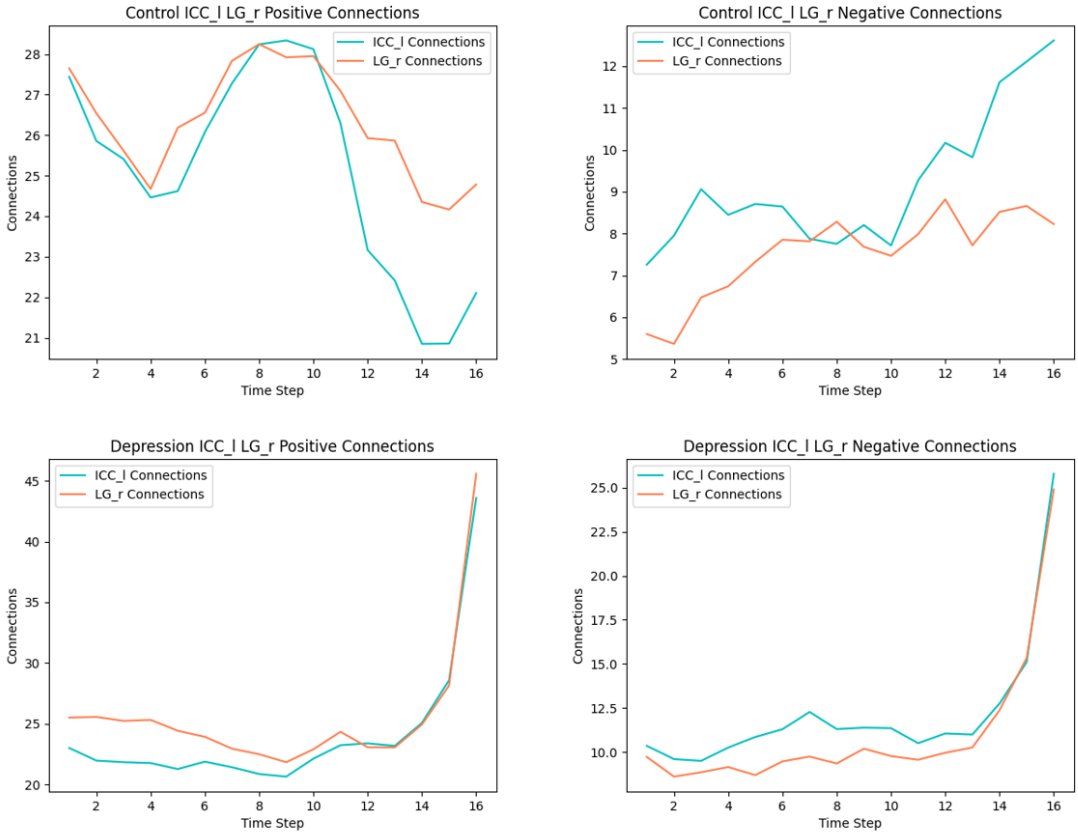

Figure 5.8: Use Case 3: Healthy control vs Depression LG_l and ICC_r dynamics.

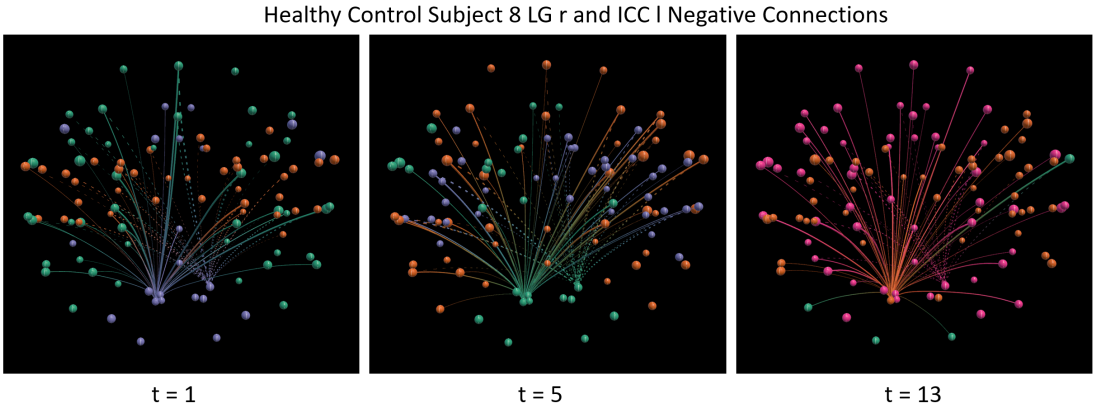

Figure 5.9: Use Case 3: Healthy Control Subject 8 LG_l and ICC_r negative connections dynamics at t = 1, 5, 13.

Chapter 6

Conclusion

We developed a pipeline to address the three research issues mentioned in the Introduction Chapter. In summary, the research issues are:

- **Research Issue 1: Visualization Research** Visualization applications development for comparing multiple dynamic connectomes.
- **Research Issue 2: Machine Learning Research** Modifying GNNs model to enable their application for time-series network datasets.
- **Research Issue 3: Neuroscience Research** Explain the machine learning model using a mask mechanism.

The pipeline consists of two visualization tools, a novel temporal graph neural network model and a mask mechanism for analyzing temporal connectome data. Our pipeline can not only yield new hypotheses for various temporal connectomes, but also enable neuroscientists for hypotheses verification. We demonstrate three use cases to show the

effectiveness of our pipeline.

Our visualization tools are designed for exploration, comparison and analysis of dynamic brain networks. The two visualization tools are described in Chapter 2 and Chapter 3, addressing research issue 1. Our tool helps clinical neuroscientists to form new hypothesis about temporal connectivities in depression patients. We introduce a novel temporal graph neural network for extracting temporal features from dynamic connectomes. This contribution is related to research issue 2 addressed in Chapter 4. The features are used for classification of healthy vs mental disorder participants or pre vs post treatments. Our network classifies remitted depression group from healthy control group with an accuracy of 98%. The network is also trained to classify pre and post R-CBT treatment connectomes with 88% accuracy. Using a mask generator, we are able to explain the decisions made by our temporal GNN model. This contribution is related to research issue 3 addressed in Chapter 4. The mask is used to sort the brain regions based on the difference between the two groups. Our findings align closely with the recent depression and R-CBT treatment studies conducted by neuroscientists based on functional connectome. Section 5.1 and 5.2 in Chapter 5 show examples of using our pipeline to analyze the remitted depression patients brain dynamics comparing with control group and analyze the effectiveness of R-CBT treatment. We identify similar brain regions using a similarity metrics on the node feature representation, enabling neuroscientists to compare similar region within connectome or across multiple connectomes. Section 5.3 showed an example of using brain region similarity features to check the different dynamic connectivities between regions.

6.1 Future Work

Our machine learning model and explainable mask can be used beyond depression studies to highlight the differences in brain regions. Our model can also act as dimensional reduction techniques extracting feature representation for dynamic connectomes. Our contributions such as graph level recurrent connection and encoding of graph structures into node features are useful in other domains such as social network and transportation analysis where explainable mechanism of model is crucial in deploying the system in real-world scenarios. Our visualization platform can also potentially supports non medical temporal network data such as geometric structure of word embeddings. With our novel overlay comparison view, we could see how the context of words change over time based on its neighboring words.

Bibliography

[1] Jae-wook Ahn, Meirav Taieb-Maimon, Awalin Sopan, Catherine Plaisant, and Ben Shneiderman. Temporal visualization of social network dynamics: Prototypes for nation of neighbors. In *International Conference on Social Computing, Behavioral-Cultural Modeling, and Prediction*, pages 309–316. Springer, 2011.

[2] A. K. Al-Awami, J. Beyer, H. Strobelt, N. Kasthuri, J. W. Lichtman, H. Pfister, and M. Hadwiger. Neurolines: A subway map metaphor for visualizing nanoscale neuronal connectivity. *IEEE Transactions on Visualization and Computer Graphics*, 20(12):2369–2378, 2014.

[3] Basak Alper, Benjamin Bach, Nathalie Henry Riche, Tobias Isenberg, and Jean-Daniel Fekete. Weighted graph comparison techniques for brain connectivity analysis. In *Proceedings of the ACM SIGCHI Conference on Human Factors in Computing Systems*, pages 483–492, 2013.

[4] Elena A Allen, Eswar Damaraju, Sergey M Plis, Erik B Erhardt, Tom Eichele, and Vince D Calhoun. Tracking whole-brain connectivity dynamics in the resting state. *Cerebral Cortex*, page bhs352, 2012.

[5] Elena A Allen, Eswar Damaraju, Sergey M Plis, Erik B Erhardt, Tom Eichele, and Vince D Calhoun. Tracking whole-brain connectivity dynamics in the resting state. *Cerebral cortex*, 24(3):663–676, 2014.

[6] Xerxes Arsiwalla, Riccardo Zucca, Alberto Betella, David Dalmazzo, Pedro Omedas, Gustavo Deco, and Paul Verschure. Network dynamics with brainx3: A large-scale simulation of the human brain network with real-time interaction. *Frontiers in Neuroinformatics*, 9, 02 2015.

[7] Xerxes D Arsiwalla, Riccardo Zucca, Alberto Betella, Enrique Martinez, David Dalmazzo, Pedro Omedas, Gustavo Deco, and Paul FMJ Verschure. Network dynamics with BrainX3: A large-scale simulation of the human brain network with real-time interaction. *Frontiers in Neuroinformatics*, 9, 2015.

[8] Benjamin Bach, Emmanuel Pietriga, and Jean-Daniel Fekete. Graphdiaries: Animated transitions andtemporal navigation for dynamic networks. *IEEE transactions on visualization and computer graphics*, 20(5):740–754, 2013.

[9] Benjamin Bach, Conglei Shi, Nicolas Heulot, Tara Madhyastha, Tom Grabowski, and Pierre Dragicevic. Time curves: Folding time to visualize patterns of temporal evolution in data. *IEEE transactions on visualization and computer graphics*, 22(1):559–568, 2015.

[10] Fabian Beck, Michael Burch, Stephan Diehl, and Daniel Weiskopf. A taxonomy and

survey of dynamic graph visualization. *Computer Graphics Forum*, 36(1):133—159, 2017.

[11] Marc G Berman, Scott Peltier, Derek Evan Nee, Ethan Kross, Patricia J Deldin, and John Jonides. Depression, rumination and the default network. *Social Cognitive and Affective Neuroscience*, 6(5):548–555, 2010.

[12] Ed Bullmore and Olaf Sporns. Complex brain networks: graph theoretical analysis of structural and functional systems. *Nature reviews neuroscience*, 10(3):186–198, 2009.

[13] Katie L Burkhouse, Rachel H Jacobs, Amy T Peters, Olu Ajilore, Edward R Watkins, and Scott A Langenecker. Neural correlates of rumination in adolescents with remitted major depressive disorder and healthy controls. *Cognitive, Affective, & Behavioral Neuroscience*, 17(2):394–405, 2017.

[14] Benson Chen, Gary Bécigneul, Octavian-Eugen Ganea, Regina Barzilay, and Tommi Jaakkola. Optimal transport graph neural networks. *arXiv preprint arXiv:2006.04804*, 2020.

[15] Mark Cheung and José MF Moura. Graph neural networks for covid-19 drug discovery. In *2020 IEEE International Conference on Big Data (Big Data)*, pages 5646–5648. IEEE, 2020.

[16] Giorgio Conte, Allen Ye, Angus Forbes, Olusola Ajilore, and Alex Leow. BRAIN-

trinsic: A VR-compatible tool for exploring intrinsic topologies of the human brain connectome. In *Brain Informatics and Health*, pages 67–76. 2015.

[17] Michael de Ridder, Karsten Klein, and Jinman Kim. TemporalTracks: Visual analytics for exploration of 4D fMRI time-series coactivation. In *Proceedings of the ACM Computer Graphics International Conference*, pages 13:1–6, 2017.

[18] Liangwei Fan, Jianpo Su, Jian Qin, Dewen Hu, and Hui Shen. A deep network model on dynamic functional connectivity with applications to gender classification and intelligence prediction. *Frontiers in neuroscience*, page 881, 2020.

[19] Wenqi Fan, Yao Ma, Qing Li, Yuan He, Eric Zhao, Jiliang Tang, and Dawei Yin. Graph neural networks for social recommendation. In *The world wide web conference*, pages 417–426, 2019.

[20] Ning Fang and Zongqian Zhan. High-resolution optical flow and frame-recurrent network for video super-resolution and deblurring. *Neurocomputing*, 2022.

[21] Paolo Federico, Wolfgang Aigner, Silvia Miksch, Florian Windhager, and Lukas Zenk. A visual analytics approach to dynamic social networks. In *Proceedings of the 11th International Conference on Knowledge Management and Knowledge Technologies*, pages 1–8, 2011.

[22] Emily S Finn, Xilin Shen, Dustin Scheinost, Monica D Rosenberg, Jessica Huang, Marvin M Chun, Xenophon Papademetris, and R Todd Constable. Functional con-

nectome fingerprinting: identifying individuals using patterns of brain connectivity. *Nature neuroscience*, 18(11):1664–1671, 2015.

[23] Angus G. Forbes, Javier Villegas, Kyle Almryde, and Elena Plante. A stereoscopic system for viewing the temporal evolution of brain activity clusters in response to linguistic stimuli. In *Stereoscopic Displays and Applications XXV*, pages 90110I–1–7. Vol. 9011 of the Proceedings of SPIE-IS&T Electronic Imaging, 2014.

[24] Takanori Fujiwara, Jia-Kai Chou, Andrew M McCullough, Charan Ranganath, and Kwan-Liu Ma. A visual analytics system for brain functional connectivity comparison across individuals, groups, and time points. In *2017 IEEE Pacific Visualization Symposium (PacificVis)*, pages 250–259. IEEE, 2017.

[25] Johnson J GadElkarim, Olusola Ajilore, Dan Schonfeld, Liang Zhan, Paul M Thompson, Jamie D Feusner, Anand Kumar, Lori L Altshuler, and Alex D Leow. Investigating brain community structure abnormalities in bipolar disorder using path length associated community estimation. *Human Brain Mapping*, 35(5):2253–2264, 2014.

[26] Florian Ganglberger, Nicolas Swoboda, Lisa Frauenstein, Joanna Kaczanowska, Wulf Haubensak, and Katja Bühler. BrainTrawler: A visual analytics framework for iterative exploration of heterogeneous big brain data. *Computers & Graphics*, 82:304–320, 2019.

[27] Caleb Geniesse, Olaf Sporns, Giovanni Petri, and Manish Saggar. Generating dy-

namical neuroimaging spatiotemporal representations (dyneusr) using topological data analysis. *Network neuroscience*, 3(3):763–778, 2019.

[28] Stephan Gerhard, Alessandro Daducci, Alia Lemkaddem, Reto Meuli, Jean-Philippe Thiran, and Patric Hagmann. The Connectome Viewer Toolkit: An open source framework to manage, analyze, and visualize connectomes. *Frontiers in Neuroinformatics*, 5:3, 2011.

[29] Michael Gleicher, Danielle Albers, Rick Walker, Ilir Jusufi, Charles D Hansen, and Jonathan C Roberts. Visual comparison for information visualization. *Information Visualization*, 10(4):289–309, 2011.

[30] Yue Gu, Ying Lin, Liangliang Huang, Junji Ma, Jinbo Zhang, Yu Xiao, Zhengjia Dai, and Alzheimer's Disease Neuroimaging Initiative. Abnormal dynamic functional connectivity in alzheimer's disease. *CNS neuroscience & therapeutics*, 26(9):962–971, 2020.

[31] Bin He, Yakang Dai, Laura Astolfi, Fabio Babiloni, Han Yuan, and Lin Yang. eConnectome: A MATLAB toolbox for mapping and imaging of brain functional connectivity. *Journal of Neuroscience Methods*, 195(2):261–269, 2011.

[32] Yang Hu, Haoxuan You, Zhecan Wang, Zhicheng Wang, Erjin Zhou, and Yue Gao. Graph-mlp: node classification without message passing in graph. *arXiv preprint arXiv:2106.04051*, 2021.

[33] R Matthew Hutchison, Thilo Womelsdorf, Elena A Allen, Peter A Bandettini,

Vince D Calhoun, Maurizio Corbetta, Stefania Della Penna, Jeff H Duyn, Gary H Glover, Javier Gonzalez-Castillo, et al. Dynamic functional connectivity: promise, issues, and interpretations. *NeuroImage*, 80:360–378, 2013.

[34] R Matthew Hutchison, Thilo Womelsdorf, Joseph S Gati, Stefan Everling, and Ravi S Menon. Resting-state networks show dynamic functional connectivity in awake humans and anesthetized macaques. *Human Brain Mapping*, 34(9):2154–2177, 2013.

[35] Andrei Irimia, Micah C Chambers, Carinna M Torgerson, and John D Van Horn. Circular representation of human cortical networks for subject and population-level connectomic visualization. *Neuroimage*, 60(2):1340–1351, 2012.

[36] Roselinde H Kaiser, Susan Whitfield-Gabrieli, Daniel G Dillon, Franziska Goer, Miranda Beltzer, Jared Minkel, Moria Smoski, Gabriel Dichter, and Diego A Pizzagalli. Dynamic resting-state functional connectivity in major depression. *Neuropsychopharmacology*, 41(7):1822–1830, 2016.

[37] Jeremy Kawahara, Colin J Brown, Steven P Miller, Brian G Booth, Vann Chau, Ruth E Grunau, Jill G Zwicker, and Ghassan Hamarneh. Brainnetcnn: Convolutional neural networks for brain networks; towards predicting neurodevelopment. *NeuroImage*, 146:1038–1049, 2017.

[38] Johnson JG Keiriz, Liang Zhan, Olusola Ajilore, Alex D Leow, and Angus G

Forbes. Neurocave: A web-based immersive visualization platform for exploring connectome datasets. *Network Neuroscience*, 2(3):344–361, 2018.

[39] Heetae Kim and Sang Hoon Lee. Relational flexibility of network elements based on inconsistent community detection. *arXiv:1904.05523*, 2019.

[40] Bonnie Klimes-Dougan, Melinda Westlund Schreiner, Michelle Thai, Meredith Gunlicks-Stoessel, Kristina Reigstad, and Kathryn R Cullen. Neural and neuroendocrine predictors of pharmacological treatment response in adolescents with depression: A preliminary study. *Progress in neuro-psychopharmacology and biological psychiatry*, 81:194–202, 2018.

[41] Ernst HW Koster, Evi De Lissnyder, Nazanin Derakshan, and Rudi De Raedt. Understanding depressive rumination from a cognitive science perspective: The impaired disengagement hypothesis. *Clinical Psychology Review*, 31(1):138–145, 2011.

[42] Aaron Kucyi and Karen D Davis. The dynamic pain connectome. *Trends in Neurosciences*, 38(2):86–95, 2015.

[43] Roan A LaPlante, Linda Douw, Wei Tang, and Steven M Stufflebeam. The connectome visualization utility: Software for visualization of human brain networks. *PLOS ONE*, 9(12):e113838, 2014.

[44] Wei Liao, Guo-Rong Wu, Qiang Xu, Gong-Jun Ji, Zhiqiang Zhang, Yu-Feng Zang,

and Guangming Lu. DynamicBC: A MATLAB toolbox for dynamic brain connectome analysis. *Brain Connectivity*, 4(10):780–790, 2014.

[45] Xuhong Liao, Miao Cao, Mingrui Xia, and Yong He. Individual differences and time-varying features of modular brain architecture. *Neuroimage*, 152:94–107, 2017.

[46] Chun-Hong Liu, Xin Ma, Lu-Ping Song, Li-Rong Tang, Bin Jing, Yu Zhang, Feng Li, Zhen Zhou, Jin Fan, and Chuan-Yue Wang. Alteration of spontaneous neuronal activity within the salience network in partially remitted depression. *Brain research*, 1599:93–102, 2015.

[47] Mary-Ellen Lynall, Danielle S Bassett, Robert Kerwin, Peter J McKenna, Manfred Kitzbichler, Ulrich Muller, and Ed Bullmore. Functional connectivity and brain networks in schizophrenia. *Journal of Neuroscience*, 30(28):9477–9487, 2010.

[48] Chihua Ma, Angus G. Forbes, Daniel A. Llano, Tanya Berger-Wolf, and Robert V. Kenyon. SwordPlots: Exploring neuron behavior within dynamic communities of brain networks. *Journal of Imaging Science and Technology*, 60(1):10405–1–13, 2016.

[49] Chihua Ma, Robert V. Kenyon, Angus G. Forbes, Tanya Berger-Wolf, Bernard J. Slater, and Daniel A. Llano. Visualizing dynamic brain networks using an animated dual-representation. In *Proceedings of the Eurographics Conference on Visualization (EuroVis)*, pages 73–77, 2015.

[50] Chihua Ma, Filippo Pellolio, Daniel A Llano, Kevin Ambrose Stebbings, Robert V

Kenyon, and G Elisabeta Marai. RemBrain: Exploring dynamic biospatial networks with mosaic matrices and mirror glyphs. *Journal of Imaging Science and Technology*, 61(6):060404–1–13, 2018.

[51] Qing Ma, Yanqing Tang, Fei Wang, Xuhong Liao, Xiaowei Jiang, Shengnan Wei, Andrea Mechelli, Yong He, and Mingrui Xia. Transdiagnostic dysfunctions in brain modules across patients with schizophrenia, bipolar disorder, and major depressive disorder: a connectome-based study. *Schizophrenia Bulletin*, 46(3):699–712, 2020.

[52] Daniel S Margulies, Joachim Böttger, Aimi Watanabe, and Krzysztof J Gorgolewski. Visualizing the human connectome. *NeuroImage*, 80:445–461, 2013.

[53] Kate Brody Nooner, Stanley J Colcombe, Russell H Tobe, Maarten Mennes, Melissa M Benedict, Alexis L Moreno, Laura J Panek, Shaquanna Brown, Stephen T Zavitz, Qingyang Li, et al. The nki-rockland sample: a model for accelerating the pace of discovery science in psychiatry. *Frontiers in Neuroscience*, 6:152, 2012.

[54] Di Peng, Wei Tian, Binbin Lu, and Min Zhu. Dmnevis: A novel visual approach to explore evolution of dynamic multivariate network. In *2018 IEEE International Conference on Systems, Man, and Cybernetics (SMC)*, pages 4304–4311. IEEE, 2018.

[55] Hanspeter Pfister, Verena Kaynig, Charl P Botha, Stefan Bruckner, Vincent J

Dercksen, Hans-Christian Hege, and Jos BTM Roerdink. Visualization in connectomics. In *Scientific Visualization*, pages 221–245. Springer, 2014.

[56] Chau Pham. Graph convolutional networks (gcn), Feb 2021.

[57] Hugo Romat, Caroline Appert, Benjamin Bach, Nathalie Henry-Riche, and Emmanuel Pietriga. Animated edge textures in node-link diagrams: A design space and initial evaluation. In *Proceedings of the ACM SIGCHI Conference on Human Factors in Computing Systems*, pages 187:1–13, 2018.

[58] Sébastien Rufiange and Michael J McGuffin. Diffani: Visualizing dynamic graphs with a hybrid of difference maps and animation. *IEEE Transactions on Visualization and Computer Graphics*, 19(12):2556–2565, 2013.

[59] Mehdi SM Sajjadi, Raviteja Vemulapalli, and Matthew Brown. Frame-recurrent video super-resolution. In *Proceedings of the IEEE Conference on Computer Vision and Pattern Recognition*, pages 6626–6634, 2018.

[60] Benjamin Sanchez-Lengeling, Emily Reif, Adam Pearce, and Alexander B. Wiltschko. A gentle introduction to graph neural networks, Sep 2021.

[61] Ni Shu, Yunyun Duan, Mingrui Xia, Menno M Schoonheim, Jing Huang, Zhuoqiong Ren, Zheng Sun, Jing Ye, Huiqing Dong, Fu-Dong Shi, et al. Disrupted topological organization of structural and functional brain connectomes in clinically isolated syndrome and multiple sclerosis. *Scientific reports*, 6(1):1–11, 2016.

[62] Olaf Sporns, Giulio Tononi, and Rolf Kötter. The human connectome: a structural description of the human brain. *PLoS computational biology*, 1(4), 2005.

[63] John Thompson, JoAnn Kuchera-Morin, Marcos Novak, Dan Overholt, Lance Putnam, Graham Wakefield, and Wesley Smith. The AlloBrain: An interactive, stereographic, 3D audio, immersive virtual world. *International Journal of Human-Computer Studies*, 67(11):934–946, 2009.

[64] Wendy Treynor, Richard Gonzalez, and Susan Nolen-Hoeksema. Rumination reconsidered: A psychometric analysis. *Cognitive therapy and research*, 27(3):247–259, 2003.

[65] David C Van Essen, Stephen M Smith, Deanna M Barch, Timothy EJ Behrens, Essa Yacoub, Kamil Ugurbil, Wu-Minn HCP Consortium, et al. The wu-minn human connectome project: an overview. *Neuroimage*, 80:62–79, 2013.

[66] K Wang, D Wei, J Yang, P Xie, X Hao, and J Qiu. Individual differences in rumination in healthy and depressive samples: Association with brain structure, functional connectivity and depression. *Psychological Medicine*, 45(14):2999–3008, 2015.

[67] Kun Wang, Meng Liang, Liang Wang, Lixia Tian, Xinqing Zhang, Kuncheng Li, and Tianzi Jiang. Altered functional connectivity in early alzheimer's disease: A resting-state fmri study. *Human brain mapping*, 28(10):967–978, 2007.

[68] Ed Watkins, Jan Scott, Janet Wingrove, Katharine Rimes, Neil Bathurst, Herbert

Steiner, Sandra Kennell-Webb, Michelle Moulds, and Yanni Malliaris. Rumination-focused cognitive behaviour therapy for residual depression: A case series. *Behaviour Research and Therapy*, 45(9):2144–2154, 2007.

[69] Sarah Weber, Erik Johnsen, Rune A Kroken, Else-Marie Løberg, Sevdalina Kandilarova, Drozdstoy Stoyanov, Kristiina Kompus, and Kenneth Hugdahl. Dynamic functional connectivity patterns in schizophrenia and the relationship with hallucinations. *Frontiers in psychiatry*, 11:227, 2020.

[70] John E Wenskovitch, Leonard A Harris, Jose-Juan Tapia, James R Faeder, and G Elisabeta Marai. Mosbie: a tool for comparison and analysis of rule-based biochemical models. *BMC bioinformatics*, 15(1):316, 2014.

[71] Lirong Wu and Stan Z Li. Beyond message passing paradigm: Training graph data with consistency constraints. 2021.

[72] Mingrui Xia, Jinhui Wang, and Yong He. BrainNet Viewer: A network visualization tool for human brain connectomics. *PLOS ONE*, 8(7):e68910, 2013.

[73] Mengqi Xing, Olusola Ajilore, Ouri Wolfson, Christopher Abbott, Annmarie MacNamara, Reza Tadayonnejad, Angus G. Forbes, K. Luan Phan, Heide Klumpp, and Alex Leow. Thought chart: Tracking dynamic EEG brain connectivity with unsupervised manifold learning. In *Brain Informatics and Health*, pages 149–157. 2016.

[74] Mengqi Xing, Hyekyoung Lee, Zachery Morrissey, Moo K Chung, K Luan Phan,

Heide Klumpp, Alex Leow, and Olusola Ajilore. Altered dynamic electroencephalography connectome phase-space features of emotion regulation in social anxiety. *NeuroImage*, 186:338–349, 2019.

[75] Baoyu Yan, Xiaopan Xu, Mengwan Liu, Kaizhong Zheng, Jian Liu, Jianming Li, Lei Wei, Binjie Zhang, Hongbing Lu, and Baojuan Li. Quantitative identification of major depression based on resting-state dynamic functional connectivity: a machine learning approach. *Frontiers in neuroscience*, 14:191, 2020.

[76] Chao-Gan Yan, Xiao Chen, Le Li, Francisco Xavier Castellanos, Tong-Jian Bai, Qi-Jing Bo, Jun Cao, Guan-Mao Chen, Ning-Xuan Chen, Wei Chen, et al. Reduced default mode network functional connectivity in patients with recurrent major depressive disorder. *Proceedings of the National Academy of Sciences*, 116(18):9078–9083, 2019.

[77] Xinsong Yang, Lei Shi, Madelaine Daianu, Hanghang Tong, Qingsong Liu, and Paul Thompson. Blockwise human brain network visual comparison using nodetrix representation. *IEEE transactions on visualization and computer graphics*, 23(1):181–190, 2016.

[78] Allen Q. Ye, Olusola Ajilore, Giorgio Conte, Johnson GadElkarim, Galen Thomas-Ramos, Liang Zhan, Shaolin Yang, Anand Kumar, Richard L Magin, Angus G Forbes, and Alex D Leow. The intrinsic geometry of the human brain connectome. *Brain Informatics*, 2(4):197–210, 2015.

[79] Liang Zhan, Lisanne Michelle Jenkins, Ouri Wolfson, Johnson J. GadElkarim, Kevin Nocito, Paul M Thompson, Olusola Ajilore, Moo K Chung, and Alex D. Leow. The significance of negative correlations in brain connectivity. *Journal of Comparative Neurology*, 525(15):3251—-3265, 2017.

[80] Xueling Zhu, Fulai Yuan, Gaofeng Zhou, Jilin Nie, Dongcui Wang, Ping Hu, Lirong Ouyang, Lingyu Kong, and Weihua Liao. Cross-network interaction for diagnosis of major depressive disorder based on resting state functional connectivity. *Brain Imaging and Behavior*, 15(3):1279–1289, 2021.

Appendix A

Brain Similarity on Group Level for Healthy Control and Remitted Depression Patients

	Healthy Control Similar Brain Regions			Depression Patients Similar Brain Regions		
Regions	**Region 1**	**Region 2**	**Region 3**	**Region 1**	**Region 2**	**Region 3**
FP_r	SFG_r	MidFG_r	PaCiG_r	sLOC_r	MidFG_r	SPL_l
FP_l	SFG_l	pMTG_l	PaCiG_l	SFG_l	pMTG_l	aITG_l
IC_r	PT_l	FO_r	PO_l	IC_l	FO_r	FO_l
IC_l	PP_r	PP_l	HG_l	IC_r	Putamen_l	FO_l
SFG_r	FP_r	PaCiG_r	toMTG_r	SFG_l	pSTG_l	aITG_r
SFG_l	FP_l	pMTG_l	PaCiG_l	SFG_r	FP_l	aITG_r
MidFG_r	FP_r	SFG_l	pITG_l	SPL_l	sLOC_r	FP_r
MidFG_l	SFG_l	Caudate_r	AG_r	toITG_l	pITG_l	SPL_l
IFG_tri_r	TP_r	IFG_oper_r	aSTG_l	IFG_oper_r	Putamen_r	pSTG_r
IFG_tri_l	pITG_l	IFG_oper_l	pITG_r	toMTG_l	pSMG_l	MidFG_l
IFG_oper_r	IFG_tri_r	toITG_r	SPL_r	IFG_tri_r	toMTG_r	IFG_oper_l
IFG_oper_l	IFG_tri_l	toMTG_r	aSTG_r	toMTG_r	pSTG_l	FOrb_l
PreCG_r	PostCG_r	PreCG_l	PostCG_l	PreCG_l	PostCG_r	PostCG_l
PreCG_l	PreCG_r	PostCG_r	PostCG_l	PreCG_r	PostCG_r	PostCG_l
TP_r	IFG_tri_r	FOrb_l	aSTG_l	pSTG_r	Amygdala_r	PaCiG_l

Table A.1 continued from previous page

TP_l	FOrb_r	FOrb_l	Amygdala_r	Hippocampus_l	aSTG_l	Amygdala_l
aSTG_r	pSTG_r	toMTG_r	IFG_oper_l	PP_l	SubCalC	Accumbens_r
aSTG_l	TP_r	Amygdala_r	IFG_tri_r	Amygdala_l	TP_l	pSTG_l
pSTG_r	aSTG_r	HG_r	pSTG_l	TP_r	Amygdala_r	HG_r
pSTG_l	IFG_tri_l	pSTG_r	TP_l	aSTG_l	SFG_r	aITG_l
aMTG_r	MedFC	aPaHC_l	pMTG_l	aPaHC_l	Hippocampus_l	aITG_r
aMTG_l	SubCalC	aITG_r	aITG_l	aITG_l	Precuneous	pMTG_l
pMTG_r	FP_l	pITG_r	MedFC	toMTG_r	aITG_r	Amygdala_l
pMTG_l	SFG_l	FP_l	PaCiG_l	aITG_l	AG_l	FP_l
toMTG_r	IFG_oper_l	aSTG_r	aTFusC_l	IFG_oper_l	Amygdala_l	pMTG_r
toMTG_l	FO_l	aITG_l	MidFG_l	pSMG_l	IFG_tri_l	AG_l
aITG_r	pPaHC_r	pPaHC_l	aMTG_l	aPaHC_l	SFG_r	SFG_l
aITG_l	SubCalC	AG_l	aMTG_l	pMTG_l	pSTG_l	aITG_r
pITG_r	FOrb_r	pITG_l	IFG_tri_l	pTFusC_r	AG_r	pTFusC_l
pITG_l	IFG_tri_l	toITG_l	pITG_r	toITG_l	MidFG_l	SPL_l
toITG_r	pTFusC_r	SPL_l	IFG_oper_r	sLOC_l	pITG_l	FP_r
toITG_l	pITG_l	IFG_tri_l	aTFusC_l	MidFG_l	pITG_l	SPL_l
PostCG_r	PreCG_r	PostCG_l	PreCG_l	PostCG_l	PreCG_l	PreCG_r
PostCG_l	PostCG_r	PreCG_r	PreCG_l	PostCG_r	PreCG_l	PreCG_r
SPL_r	iLOC_l	iLOC_r	IFG_oper_r	aSMG_r	aSMG_l	pTFusC_l
SPL_l	toITG_r	pTFusC_r	aSTG_l	MidFG_r	toITG_l	pITG_l
aSMG_r	PO_r	IFG_oper_r	PT_r	aSMG_l	SPL_r	IFG_oper_r
aSMG_l	pSMG_r	aSMG_r	PO_r	aSMG_r	SPL_r	pSMG_r
pSMG_r	aSMG_l	toMTG_r	aSMG_r	pSMG_l	toMTG_l	AG_l
pSMG_l	MidFG_l	AG_r	Caudate_l	toMTG_l	pSMG_r	IFG_tri_l
AG_r	MidFG_l	aITG_r	AG_l	aTFusC_l	pITG_r	aTFusC_r
AG_l	aITG_l	AG_r	MidFG_l	pMTG_l	toMTG_l	pSMG_l
sLOC_r	aTFusC_r	pTFusC_r	aTFusC_l	MidFG_r	FP_r	pTFusC_l
sLOC_l	MidFG_l	pPaHC_r	pPaHC_l	pITG_l	toITG_r	toITG_l
iLOC_r	iLOC_l	pTFusC_l	TOFusC_l	TOFusC_r	iLOC_l	OFusG_r
iLOC_l	iLOC_r	pTFusC_l	SPL_r	TOFusC_l	iLOC_r	aITG_r
ICC_r	Cuneal_r	SCC_l	Cuneal_l	SCC_r	ICC_l	SCC_l
ICC_l	SCC_r	Cuneal_r	SCC_l	ICC_r	LG_r	SCC_r
MedFC	aPaHC_l	Hippocampus_l	aMTG_r	pPaHC_r	pPaHC_l	aPaHC_r
SMA_r	SMA_l	PostCG_l	PostCG_r	SMA_l	PO_r	PostCG_l
SMA_l	CO_r	SMA_r	PT_r	SMA_r	CO_l	PaCiG_r
SubCalC	aITG_l	pPaHC_r	aMTG_l	PP_l	aSTG_r	Accumbens_r
PaCiG_r	FOrb_r	FOrb_l	SFG_r	PaCiG_l	MedFC	SMA_l
PaCiG_l	SFG_l	pMTG_l	FP_l	Amygdala_r	aSTG_l	TP_l

Table A.1 continued from previous page

AC	Caudate_r	Amygdala_l	Putamen_r	Accumbens_l	PP_l	Accumbens_r
PC	Precuneous	AG_l	SubCalC	Precuneous	aMTG_l	SubCalC
Precuneous	PC	SubCalC	Cuneal_l	PC	SubCalC	aMTG_l
Cuneal_r	SCC_l	Cuneal_l	ICC_r	LG_r	ICC_l	Cuneal_l
Cuneal_l	SCC_l	Cuneal_r	ICC_r	ICC_r	Cuneal_r	SCC_r
FOrb_r	Amygdala_r	PaCiG_r	FOrb_l	Accumbens_l	FO_l	PP_r
FOrb_l	FOrb_r	PaCiG_r	TP_r	Thalamus_l	PP_r	Pallidum_l
aPaHC_r	Hippocampus_r	Amygdala_r	pTFusC_r	aPaHC_l	pPaHC_r	pPaHC_l
aPaHC_l	Hippocampus_l	MedFC	pITG_r	Hippocampus_l	aMTG_r	aITG_r
pPaHC_r	pPaHC_l	Caudate_r	SubCalC	pPaHC_l	aPaHC_r	MedFC
pPaHC_l	pPaHC_r	aITG_r	pMTG_l	pPaHC_r	aPaHC_r	MedFC
LG_r	LG_l	OP_r	OP_l	ICC_l	ICC_r	Cuneal_r
LG_l	LG_r	OP_r	OP_l	LG_r	Cuneal_r	ICC_l
aTFusC_r	aTFusC_l	aPaHC_r	pTFusC_r	aTFusC_l	pITG_r	AG_r
aTFusC_l	aTFusC_r	aPaHC_r	pTFusC_r	aTFusC_r	AG_r	SPL_l
pTFusC_r	aPaHC_r	aTFusC_r	toITG_r	pITG_r	pTFusC_l	FP_l
pTFusC_l	iLOC_r	iLOC_l	SPL_r	pTFusC_r	sLOC_r	pITG_r
TOFusC_r	TOFusC_l	iLOC_r	OFusG_l	iLOC_r	OFusG_r	TOFusC_l
TOFusC_l	TOFusC_r	iLOC_r	OFusG_l	iLOC_l	iLOC_r	TOFusC_r
OFusG_r	OFusG_l	TOFusC_l	TOFusC_r	OFusG_l	OP_r	iLOC_r
OFusG_l	OFusG_r	TOFusC_l	TOFusC_r	OFusG_r	OP_r	LG_l
FO_r	IC_r	aSTG_r	IFG_oper_l	Putamen_r	FO_l	CO_l
FO_l	Putamen_r	AC	HG_l	FOrb_r	Putamen_l	Pallidum_r
CO_r	SMA_l	PT_r	PO_r	PO_r	pSTG_r	PostCG_l
CO_l	PO_r	PT_r	CO_r	Putamen_r	HG_l	FO_r
PO_r	PT_r	CO_l	CO_r	CO_r	PT_r	pSTG_r
PO_l	PT_l	IC_r	CO_l	PT_l	HG_r	PT_r
PP_r	PP_l	IC_l	Thalamus_r	Pallidum_l	Thalamus_r	Thalamus_l
PP_l	PP_r	IC_l	Pallidum_l	aSTG_r	Accumbens_r	SubCalC
HG_r	HG_l	Putamen_r	pSTG_r	PT_r	PT_l	PO_l
HG_l	HG_r	Putamen_r	FO_l	PT_l	Pallidum_l	PO_l
PT_r	PO_r	CO_l	CO_r	HG_r	PT_l	PO_l
PT_l	PO_l	IC_r	HG_l	PO_l	HG_r	HG_l
SCC_r	ICC_l	Cuneal_r	SCC_l	ICC_r	SCC_l	ICC_l
SCC_l	Cuneal_r	Cuneal_l	ICC_r	SCC_r	ICC_r	ICC_l
OP_r	OP_l	LG_r	LG_l	OP_l	OFusG_r	OFusG_l
OP_l	OP_r	LG_r	LG_l	OP_r	AC	Cuneal_r
Thalamus_r	Caudate_r	PP_r	AC	Pallidum_l	PP_r	Caudate_r
Thalamus_l	Accumbens_l	Pallidum_l	Accumbens_r	Caudate_r	Caudate_l	PP_r

Table A.1 continued from previous page

Caudate_r	AC	Amygdala_l	pPaHC_r	Caudate_l	Thalamus_l	Pallidum_l
Caudate_l	Thalamus_l	Accumbens_l	Thalamus_r	Caudate_r	Thalamus_l	Pallidum_r
Putamen_r	FO_l	HG_r	AC	FO_r	PO_l	CO_l
Putamen_l	Pallidum_l	Pallidum_r	Accumbens_l	Pallidum_r	FO_l	PP_l
Pallidum_r	Putamen_l	Pallidum_l	Accumbens_l	Putamen_l	Caudate_l	PP_l
Pallidum_l	Putamen_l	Thalamus_l	Accumbens_l	PP_r	Caudate_r	Thalamus_r
Hippocampus_r	aPaHC_r	Amygdala_r	TP_r	aPaHC_l	TP_l	Amygdala_r
Hippocampus_l	aPaHC_l	MedFC	TP_l	TP_l	aPaHC_l	aMTG_r
Amygdala_r	FOrb_r	aPaHC_r	Hippocampus_r	Amygdala_l	PaCiG_l	TP_r
Amygdala_l	AC	Caudate_r	Putamen_r	aSTG_l	Amygdala_r	TP_l
Accumbens_r	Accumbens_l	Thalamus_l	Putamen_l	PP_l	AC	aSTG_r
Accumbens_l	Accumbens_r	Thalamus_l	Pallidum_l	FOrb_r	AC	PP_l

Table A.1: Top 3 Brain regions that have similar dynamic features based on feature representation on group level from the healthy control group and depressive group

Appendix B

Table: Anatomical Labels of Brain Regions

Brain Region Abbr.	**Brain Region Name**
FP r	Frontal pole right
FP l	Frontal pole left
IC r	Insular cortex right
IC l	Insular cortex left
SFG r	Superior frontal gyrus right
SFG l	Superior frontal gyrus left
MidFG r	Middle frontal gyrus right
MidFG l	Middle frontal gyrus left
IFG tri r	Inferior frontal gyrus, pars triangularis right
IFG tri l	Inferior frontal gyrus, pars triangularis left
IFG oper r	Inferior frontal gyrus, pars opercularis right

Brain Region Abbr.	Brain Region Name
IFG oper l	Inferior frontal gyrus, pars opercularis left
PreCG r	Precentral gyrus right
PreCG l	Precentral gyrus left
TP r	Temporal pole right
TP l	Temporal pole left
aSTG r	Superior temporal gyrus, anterior division right
aSTG l	Superior temporal gyrus, anterior division left
pSTG r	Superior temporal gyrus, posterior division right
pSTG l	Superior temporal gyrus, posterior division left
aMTG r	Middle temporal gyrus, anterior division right
aMTG l	Middle temporal gyrus, anterior division left
pMTG r	Middle temporal gyrus, posterior division right
pMTG l	Middle temporal gyrus, posterior division left
toMTG r	Middle temporal gyrus, temporooccipital part right
toMTG l	Middle temporal gyrus, temporooccipital part left
aITG r	Inferior temporal gyrus, anterior division right
aITG l	Inferior temporal gyrus, anterior division left
pITG r	Inferior temporal gyrus, posterior division right
pITG l	Inferior temporal gyrus, posterior division left
toITG r	Inferior temporal gyrus, temporooccipital part right
toITG l	Inferior temporal gyrus, temporooccipital part left
PostCG r	Postcentral gyrus right
PostCG l	Postcentral gyrus left

Brain Region Abbr.	Brain Region Name
SPL r	Superior parietal lobule right
SPL l	Superior parietal lobule left
aSMG r	Supramarginal gyrus, anterior division right
aSMG l	Supramarginal gyrus, anterior division left
pSMG r	Supramarginal gyrus, posterior division right
pSMG l	Supramarginal gyrus, posterior division left
AG r	Angular gyrus right
AG l	Angular gyrus left
sLOC r	Lateral occipital cortex, superior division right
sLOC l	Lateral occipital cortex, superior division left
iLOC r	Lateral occipital cortex, inferior division right
iLOC l	Lateral occipital cortex, inferior division left
ICC r	Intracalcarine cortex right
ICC l	Intracalcarine cortex left
MedFC	Frontal medial cortex
SMA r	Juxtapositional lobule cortex (formerly supplementary motor cortex right)
SMA l	Juxtapositional lobule cortex (formerly supplementary motor cortex left)
SubCalC	Subcallosal cortex
PaCiG r	Paracingulate gyrus right
PaCiG l	Paracingulate gyrus left
AC	Cingulate gyrus, anterior division

Brain Region Abbr.	Brain Region Name
PC	Cingulate gyrus, posterior division
Precuneus	Precuneus cortex
Cuneal r	Cuneal cortex right
Cuneal l	Cuneal cortex left
FOrb r	Frontal orbital cortex right
FOrb l	Frontal orbital cortex left
aPaHC r	Parahippocampal gyrus, anterior division right
aPaHC l	Parahippocampal gyrus, anterior division left
pPaHC r	Parahippocampal gyrus, posterior division right
pPaHC l	Parahippocampal gyrus, posterior division left
LG r	Lingual gyrus right
LG l	Lingual gyrus left
aTFusC r	Temporal fusiform cortex, anterior division right
aTFusC l	Temporal fusiform cortex, anterior division left
pTFusC r	Temporal fusiform cortex, posterior division right
pTFusC l	Temporal fusiform cortex, posterior division left
TOFusC r	Temporal occipital fusiform cortex right
TOFusC l	Temporal occipital fusiform cortex left
OFusG r	Occipital fusiform gyrus right
OFusG l	Occipital fusiform gyrus left
FO r	Frontal operculum cortex right
FO l	Frontal operculum cortex left
CO r	Central opercular cortex right

Brain Region Abbr.	Brain Region Name
CO l	Central opercular cortex left
PO r	Parietal operculum cortex right
PO l	Parietal operculum cortex left
PP r	Planum polare right
PP l	Planum polare left
HG r	Heschl's gyrus right
HG l	Heschl's gyrus left
PT r	Planum temporale right
PT l	Planum temporale left
SCC r	Supracalcarine cortex right
SCC l	Supracalcarine cortex left
OP r	Occipital pole right
OP l	Occipital pole left
Thalamus r	Thalamus right
Thalamus l	Thalamus left
Caudate r	Caudate right
Caudate l	Caudate left
Putamen r	Putamen right
Putamen l	Putamen left
Pallidum r	Pallidum right
Pallidum l	Pallidum left
Hippocampus r	Hippocampus right
Hippocampus l	Hippocampus left

Brain Region Abbr.	**Brain Region Name**
Amygdala r	Amygdala right
Amygdala l	Amygdala left
Accumbens r	Accumbens right
Accumbens l	Accumbens left

Table B.1: Anatomical Labels of Brain Regions